Supporting Information for

Phainanolide A, Highly Modified and Oxygenated Triterpenoid from *Phyllanthus hainanensis*

Yao-Yue Fan,[†] Li-She Gan,[‡] Hong-Chun Liu,[†] Heng Li,[†] Cheng-Hui Xu,[†] Jian-Ping Zuo,[†] Jian Ding,[*,†] and Jian-Min Yue[*,†]

[†]State Key Laboratory of Drug Research, Shanghai Institute of Materia Medica, Chinese Academy of Sciences, 555 Zu Chong Zhi Road, Zhangjiang Hi-Tech Park, Shanghai, 201203, People's Republic of China.

[‡]Institute of Modern Chinese Medicine, College of Pharmaceutical Sciences, Zhejiang University, Hangzhou, 310058, People's Republic of China.

List of Supporting Information

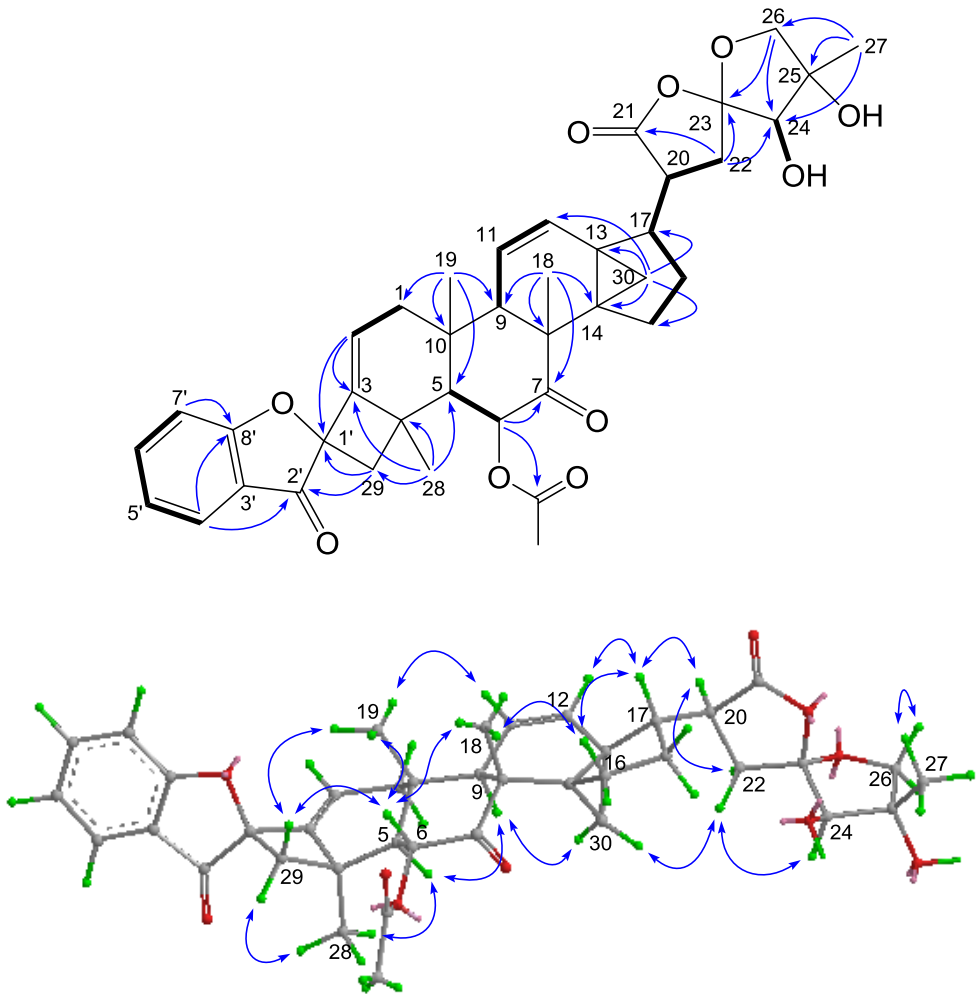

Figure S1. Key 2D NMR correlations for phainanoid G (**2**).

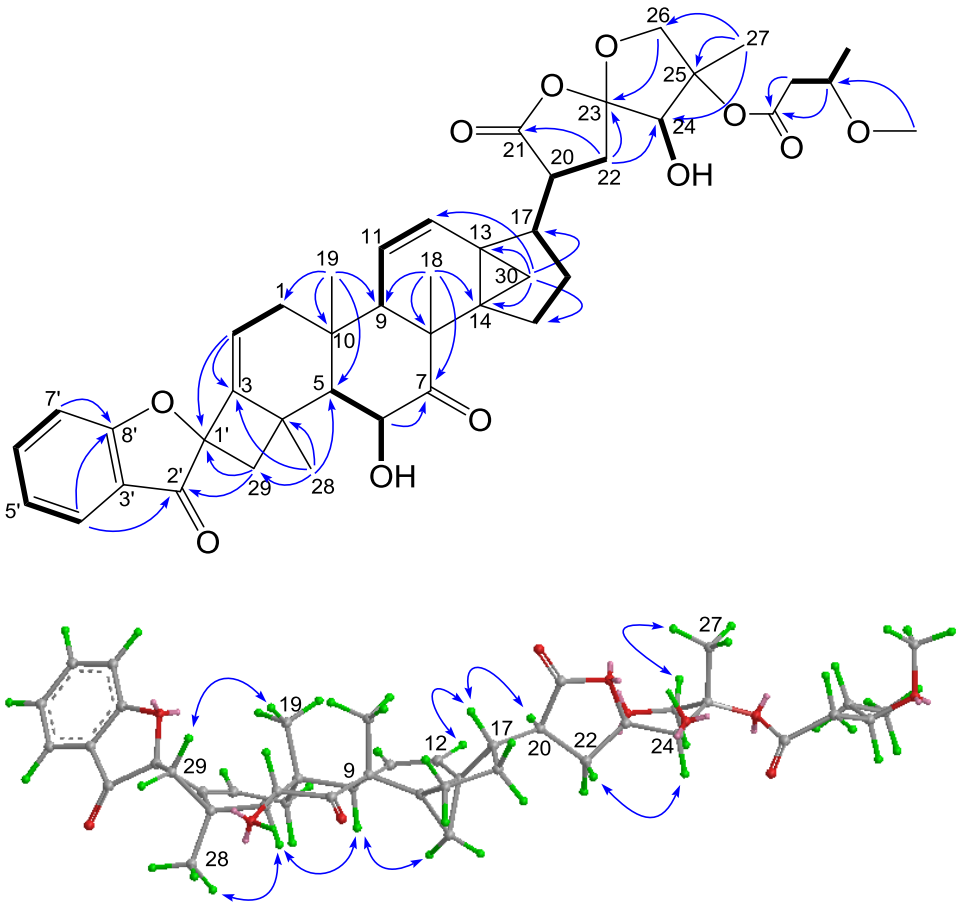

Figure S2. Key 2D NMR correlations for phainanoid H (**3**).

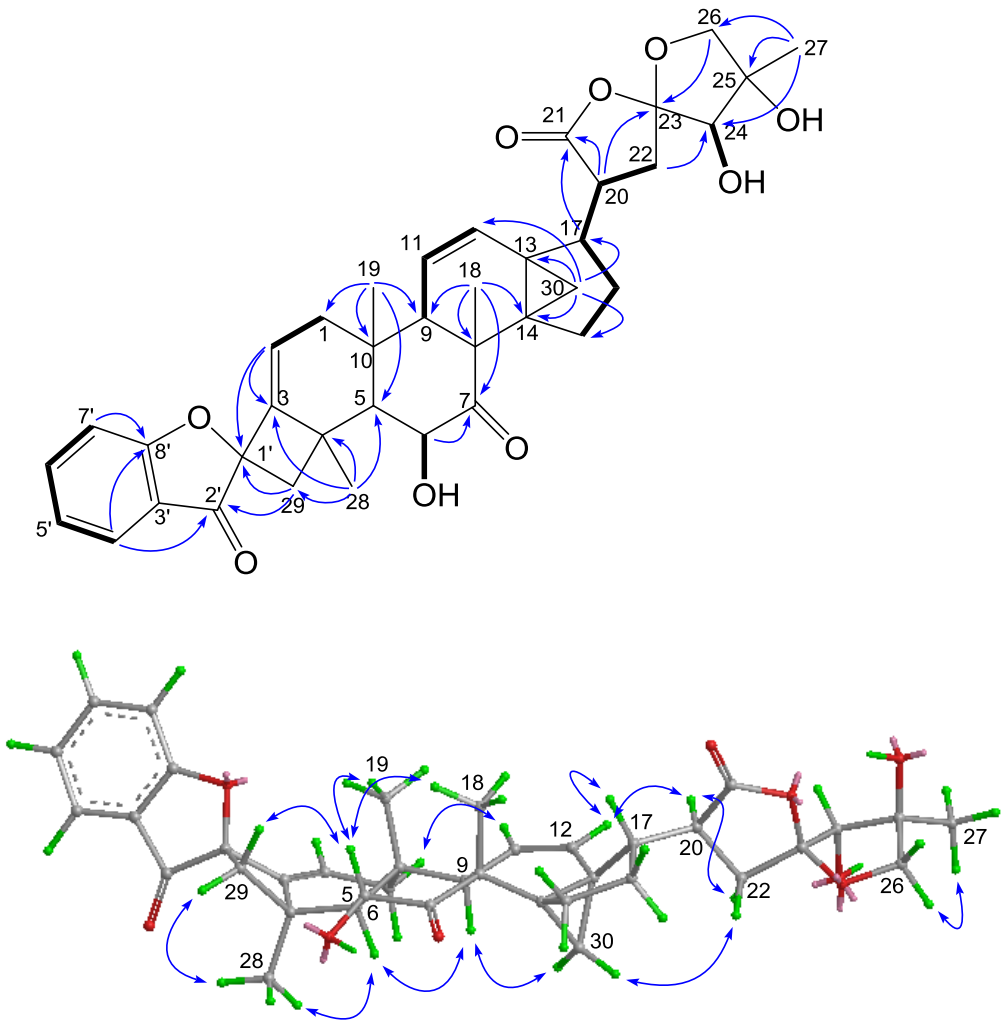

Figure S3. Key 2D NMR correlations for phainanoid I (**4**).

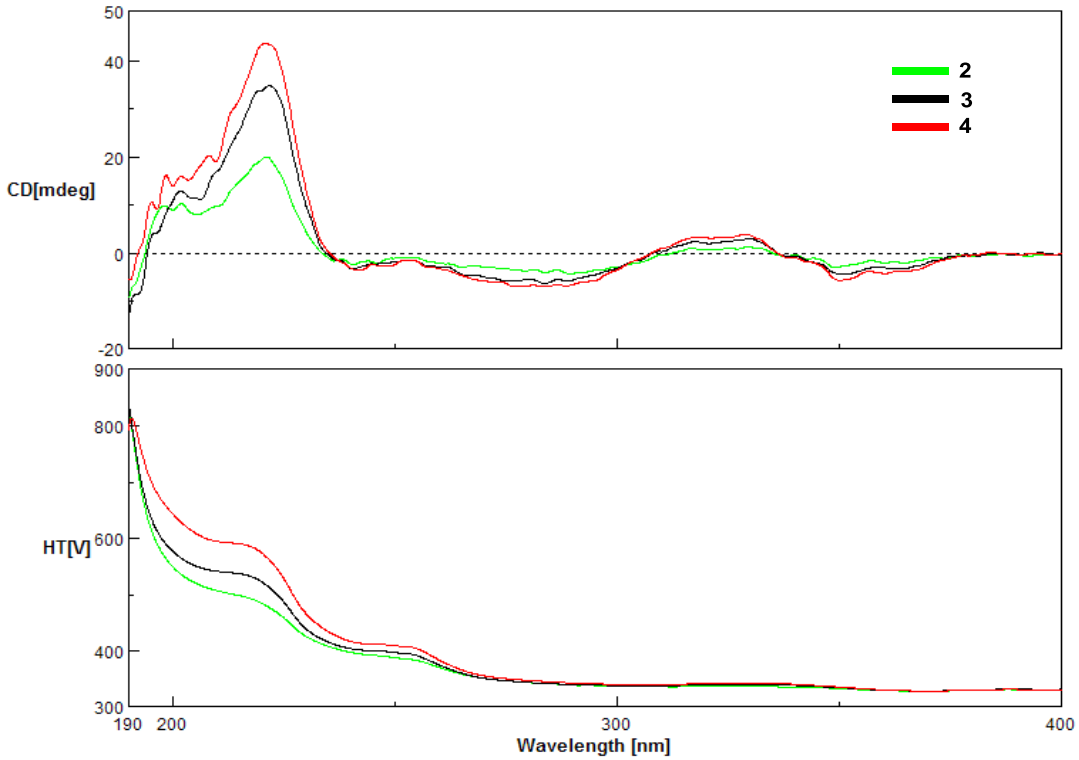

Figure S4. CD spectra of compounds **2**−**4**.

Table S1. ^{1}H NMR data ($CDCl_3$, 400 MHz) for compounds **1**–**4**.

No	**1**	**2**	**3**	**4**
1*α*	1.80 m	1.57 dd (14.7, 4.2)	1.51 dd (14.6, 4.2)	1.50 dd (14.6, 4.1)
1*β*	2.46 m	2.33 dd (14.7, 8.5)	2.26 dd (14.6, 8.4)	2.25 dd (14.6, 8.5)
2	5.92 dd (7.9, 2.4)	5.77 dd (8.5, 4.2)	5.73 dd (8.4, 4.2)	5.72 dd (8.5, 4.1)
5	1.76 d (12.9)	1.90 d (13.9)	1.53 d (13.2)	1.54 d (13.4)
6	4.56 dd (12.9, 4.4)	5.66 d (13.9)	4.67 dd (13.2, 5.0)	4.67 dd (13.4, 4.9)
9	2.04 brs	2.06 dd (2.9, 2.5)	2.03 dd (2.5, 2.8)	2.05 dd (2.9, 2.6)
11	5.43 dd (10.0, 2.4)	5.42 dd (9.9, 2.5)	5.42 dd (10.0, 2.5)	5.40 dd (10.0, 2.6)
12	6.33 dd (10.0, 2.8)	6.28 dd (9.9, 2.9)	6.27 dd (9.9, 2.8)	6.22 dd (10.0, 2.9)
15*β*	1.99 m	2.01 m	2.01 m	2.00 m
15*α*	2.20 m	2.18 m	2.20 m	2.20 m
16*α*	1.35 m	1.13 m	1.17 m	1.24 m
16*β*	1.79 m	1.70 m	1.73 m	1.85 m
17	2.60 m	2.53 m	2.54 m	2.54 m
18	1.22 s	1.27 s	1.21 s	1.22 s
19	1.16 s	1.32 s	1.29 s	1.29 s
20	2.97 dd (9.8, 5.5)	3.28 td (10.1, 5.6)	3.22 ddd (10.1, 7.4, 5.6)	2.87 ddd (9.8, 7.0, 6.1)
22	4.37 dd (9.9, 9.8)	2.35 d (10.1, 2H)	2.29 m	2.14 dd (14.0, 6.1)
22			2.39 m	2.77 dd (14.0, 9.8)
24	4.42 d (5.4)	4.04 d (10.9)	4.16 d (5.0)	3.98 brs
26*β*	4.22 d (10.1)	3.93 d (9.6)	4.06 d (10.4)	4.00 d (9.6)
26*α*	4.32 d (10.1)	3.96 d (9.6)	4.27 d (10.4)	4.07 d (9.6)
27	1.61 s	1.43 s	1.56 s	1.41 s
28	1.40 s	1.78 s	1.77 s	1.77 s
29*β*	4.18 d (9.9)	2.29 d (11.6)	2.52 d (11.6)	2.52 d (11.5)
29*α*	4.83 d (9.9)	2.49 d (11.6)	2.68 d (11.6)	2.68 d (11.5)
30a	1.05 d (6.5)	0.85 d (6.4)	0.89 d (6.3)	0.96 d (6.4)
30b	1.30 d (6.5)	1.29 d (6.4)	1.31 d (6.3)	1.40 d (6.4)
4′	7.52 d (7.0)	7.66 dd (8.1, 1.4)	7.67 dd (7.8, 1.4)	7.67 brd (7.7)
5′	7.20 m	7.09 brdd (8.1, 7.3)	7.08 brdd (7.8, 7.3)	7.08 brdd (7.7, 7.2)
6′	7.26 m	7.62 ddd (8.3, 7.3, 1.4)	7.61 ddd (8.3, 7.3, 1.4)	7.61 ddd (8.4, 7.2, 1.3)
7′	7.38 d (8.1)	7.08 brd (8.3)	7.08 brd (8.3)	7.08 brd (8.4)
10′	2.49 m (2H)			
11′	4.21 m			
12′	1.26 d (6.3)			
6-OH	3.89 d (4.4)		3.51 d (5.0)	3.51 d (4.9)
22-OH	2.36 d (9.9)			
24-OH	3.31 d (5.4)	2.04 d (10.9)	3.33 d (5.0)	2.43 brs
25-OH		1.85 brs		2.97 brs
OAc		2.18 s		
2″			2.41 m	
			2.54 m	
3″			3.75 m	
4″			1.21 d (7.7)	
3″-OMe			3.33 s	

Table S2. ^{13}C NMR Data ($CDCl_3$, 125 MHz) for compounds **1**–**4**.

Position	**1**	**2**	**3**	**4**
1	40.5	37.6	37.7	37.7
2	112.9	120.3	119.9	119.9
3	132.8	145.6	146.2	146.2
4	37.1	42.8	43.4	43.4
5	60.4	58.0	61.7	61.7
6	70.9	73.7	71.7	71.7
7	213.3	206.0	213.4	213.4
8	47.2	48.4	47.5	47.5
9	51.6	50.8	51.3	51.2
10	37.3	42.7	42.2	42.2
11	120.3	120.3	120.5	120.3
12	131.8	131.7	131.5	131.9
13	31.7	32.35	32.3	32.6
14	36.6	36.9	36.6	37.5
15	26.8	27.2	27.0	26.8
16	23.8	23.8	23.8	26.3
17	40.7	41.4	41.6	43.0
18	17.3	17.2	17.4	17.4
19	16.4	15.2	15.3	15.3
20	47.0	40.9	40.7	42.4
21	173.5	177.1	177.1	176.4
22	69.6	32.4	31.3	30.9
23	108.8	111.8	111.2	116.1
24	76.9	83.2	80.4	82.1
25	86.6	77.4	86.5	79.4
26	78.0	78.6	77.9	80.2
27	18.6	21.7	18.8	18.9
28	28.1	28.0	28.4	28.4
29	72.7	39.9	40.2	40.2
30	14.5	14.3	14.1	14.2
1′	137.1	92.6	93.0	93.0
2′	136.7	198.5	198.5	198.6
3′	121.4	120.7	120.9	120.9
4′	118.3	125.0	125.0	125.0
5′	122.7	122.2	122.1	122.1
6′	124.9	138.2	138.0	138.0
7′	111.6	113.0	112.9	112.9
8′	153.3	170.8	170.8	170.8
9′	173.7			
10′	43.4			
11′	64.5			
12′	22.8			
6-OAc		20.9		
		170.2		
1″			172.8	
2″			42.4	
3″			73.8	
4″			19.2	
3″-OCH3			56.6	

Table S3. Linear correlation coefficients R^2 and root-mean-square deviation (RMSD) analyses of the calculated and experimental ^{13}C NMR data of four model compounds.

Isomers	**1a**	**1b**	**1c**	**1d**
R^2	0.98112	0.97734	0.97875	0.97143
RMSD	10.41222	11.66796	10.52129	12.90987

Table S4. DP4+ analysis result table (Isomer 1 for **1a**, Isomer 2 for **1b**, Isomer 3 for **1c**, Isomer 4 for **1d**).

Functional		Solvent?	Basis Set			Type of Data	
mPW1PW91		Gas Phase	6-31+G(d,p)			Unscaled Shifts	
		DP4+	95.89%	0.00%	4.11%	0.00%	-
Nuclei	sp2?	xperimenta	Isomer 1	Isomer 2	Isomer 3	Isomer 4	Isomer 5
C	x	137.1	145.85315	143.00475	135.219711	136.79955	
C	x	136.7	142.97335	151.35535	152.19886	153.98665	
C	x	121.4	137.02025	136.75235	128.157317	135.05145	
C	x	118.3	136.31975	138.04365	136.656548	136.47675	
C	x	122.7	131.36905	130.34115	126.760747	129.69465	
C	x	124.9	134.25685	135.82715	135.84314	137.67695	
C	x	111.6	128.27185	125.64275	127.024457	128.57555	
C	x	153.3	155.93065	158.82685	164.067745	166.13705	
C	x	173.7	174.96765	176.91045	177.580143	178.52735	
C		43.4	46.92565	43.67835	46.3308929	43.70025	
C		64.5	76.89055	83.00425	78.1777046	86.65625	
C		22.8	23.87665	23.26725	23.8819922	25.00775	

Experimental Section

General Experimental Procedures. NMR spectra were recorded on a Bruker Avance III 500 spectrometer (Bruker Biospin Rheinstetten, Germany) with TMS as internal standard. ESIMS was measured on a Bruker Daltonics esquire 3000 plus instrument (Bruker Biospin Rheinstetten, Germany). HRESIMS was measured with a LCT Premier XE (Waters) mass spectrometer (Waters, Milford, MA, U.S.). Optical rotations were obtained on a Perkin-Elmer 341 polarimeter (Wellesley, MA, USA) at set temperature. CD spectra were obtained on a JASCO J-810 spectrometer (Shimadzu, Kyoto, Japan). UV spectra were measured on a Shimadzu UV-2550 UV-visible spectrophotometer (Shimadzu, Kyoto, Japan). IR spectra were recorded on a Perkin-Elmer 577 IR spectrometer (Wellesley, MA, USA) with KBr disks. Column chromatography was performed on silica gel (300–400 mesh). MCI gel (CHP20P, 75–150 μm, Mitsubishi Chemical Industries, Ltd.), C_{18} reversed-phase silica gel (150–200 mesh, Merck), and Sephadex LH-20 (Amersham Biosciences) were used for reverse phase column chromatography, and precoated silica gel GF254 plates (Qingdao Marine Chemical Plant, Qingdao, China) were used for thin-layer chromatography (TLC). Semi-preparative HPLC was performed on a Waters 1525 pump with a Waters 2489 detector (254 nm and 210 nm) and an YMC-Pack ODS-A column (250 × 10 mm, S-5 μm, 12 nm). All solvents were of analytical grade (Shanghai Chemical Reagents Co. Ltd., China), and solvents used for HPLC were of HPLC grade (J&K Scientific Ltd., China).

Plant Material. The entire plants of *Phyllanthus hainanensis* Merr. were collected from Hainan island, P. R. China, and were authenticated by Prof. S-M Huang, Department of Biology, Hainan University, P. R. China. A voucher specimen has been deposited in the herbarium of Shanghai Institute of Materia Medica, Chinese Academy of Sciences (accession number: Ph-2010Hn-1Y).

Extraction and Isolation. The air-dried powder of the plant material (5 kg) was percolated three times with 95% EtOH (10 L) at RT, to give 300 g of crude extract which was suspended in water (0.5 L) and partitioned successively with EtOAc (3 × 0.5 L) and *n*-BuOH (3 × 0.5 L). The EtOAc-soluble part (103 g) was fractionated by a MCI gel column eluted with MeOH/H_2O (30–100%) to give four fractions F1–F4. Fraction F2 (3 g) was extensively chromatographed over silica gel, RP-18 silica gel, and Sephadex LH-20 gel to afford mixtures of the major components, which were further purified by semi-preparative HPLC to yield compounds **1** (3.1 mg), **2** (2.2 mg), **3** (3.0 mg), and **4** (4.7 mg).

Physical constants and spectral data of 1–4

Phainanolide A (1): White amorphous solid; $[\alpha]_D^{25}$ = +41.7 (*c* = 0.10 in $CHCl_3$); ^1H and ^{13}C NMR data, see Tables S1 and S2; IR (KBr): ν_{max} = 3399 cm^{-1} (O-H), 1731, 1714 cm^{-1} (C=O); UV/Vis (EtOH): λ_{max} (log ε) = 308 (3.51), 295 (3.25), 251 (3.11), 242 (3.22) nm; CD (EtOH): λ ($\Delta\varepsilon$) = 211 (–3.70), 251 (2.67), 306 (2.81), 321 (2.45), nm; LRESI(±)MS: *m*/*z* 745.4 $[M + H]^+$, 790.2 $[M + HCO_2]^-$; HRESI(–)MS: *m*/*z* 789.3119 $[M + HCO_2]^-$ (calcd for $C_{43}H_{49}O_{14}$, 789.3122).

Phainanoid G (2): White amorphous solid; $[\alpha]_D^{25}$ = +3.3 (*c* = 0.06 in $CHCl_3$); ^1H and ^{13}C NMR data, see Tables S1 and S2; IR (KBr): ν_{max} = 3491 cm^{-1} (O-H), 1747, 1721 cm^{-1} (C=O); UV/Vis (EtOH): λ_{max} (log ε) = 215.0 (4.03), 253.2 (3.51) nm; CD (EtOH): λ ($\Delta\varepsilon$) = 221 (10.96), 241 (–1.12), 290 (–2.31), 330 (0.68), 350 (–1.52) nm; LRESI(±)MS: *m*/*z* 685.4 $[M + H]^+$, 729.5 $[M + HCO_2]^-$; HRESI(–)MS: *m*/*z* 729.2922 $[M + HCO_2]^-$ (calcd for $C_{41}H_{45}O_{12}$, 729.2911).

Phainanoid H (3): White amorphous solid; $[\alpha]_D^{25}$ = +19.1 (*c* = 0.08 in $CHCl_3$); ^1H and ^{13}C NMR data, see Tables S1 and S2; IR (KBr): ν_{max} = 3425 cm^{-1} (O-H), 1783, 1712 cm^{-1} (C=O); UV/Vis (EtOH): λ_{max} (log ε) = 219 (4.29), 253 (3.80) nm; CD (EtOH): λ ($\Delta\varepsilon$) = 222 (24.67), 241 (–2.19), 284 (–4.38), 330 (2.13), 351 (–3.09) nm; LRESI(±)MS: *m*/*z* 743.4 $[M + H]^+$, 787.9 $[M + HCO_2]^-$; HRESI(+)MS: *m*/*z* 765.3237 $[M + Na]^+$ (calcd for $C_{43}H_{50}O_{11}Na$, 765.3245).

Phainanoid I (4): White amorphous solid; $[\alpha]_D^{25}$ = –10.3 (*c* = 0.09 in $CHCl_3$); ^1H and ^{13}C NMR data, see Tables S1 and S2; IR (KBr): ν_{max} = 3438 cm^{-1} (O-H), 1765, 1712 cm^{-1} (C=O); UV/Vis (EtOH): λ_{max} (log ε) = 218 (4.08), 254 (3.58) nm; CD (EtOH): λ ($\Delta\varepsilon$) = 222 (25.36), 241 (–2.09), 284 (–4.38), 330 (2.71), 351 (–3.40) nm; LRESI(±)MS: *m/z* 643.3 $[M + H]^+$, 687.8 $[M + HCO_2]^-$; HRESI(–)MS: *m/z* 687.2826 $[M + HCO_2]^-$ (calcd for $C_{39}H_{43}O_{11}$, 687.2805).

Bioassays

Cytotoxicity

The *in vitro* cytotoxicities of all isolated compounds against HL-60 cell line were measured by using the MTT method. Briefly, test cells in culture medium 100 μL were seeded in each well of 96-well plates (Falcon, CA). Cells were treated in triplicate with 10 μL of grade concentrations of the compounds at 37 ℃. After 72 h, a 20 μL aliquot of MTT solution (5 mg/mL) was added to the wells. The cultures were incubated for another 4 h, and then 100 μL of "triplex solution" (10% SDS/5% isobutanol/10 mM HCl) was added. The plates were incubated at 37 ℃ in 5% CO_2 overnight. The OD values were measured at 570 nm by a plate reader (VERSA Max, Molecular Devices, Sunnyvale, CA). Average values determined from triplicate readings were used for the inhibitory rate calculation by the formula: $(OD_{control\ well} - OD_{treated\ well})/OD_{control\ well} - OD_{blank\ well} \times 100\%$. The IC_{50} was calculated using Logistic regression from three independent tests. Adriamycin was used as the positive control.

The *in vitro* cytotoxicities of all isolated compounds against A549 cells were evaluated by using the SRB assay. Briefly, test cells were seeded into 96-well plates (Falcon, CA) and allowed to attach overnight. The cells were treated in triplicate with 10 μL of grade concentrations of the compounds at 37 ℃ for 72 h and were then fixed with 10% trichloroacetic acid and incubated at 4 ℃ for 1 h. The culture plates were washed and dried, and then SRB solution (0.4 wt %/vol in 1% acetic acid) was added and incubated for 15 min. The culture plates were washed and dried again, the bound cell stains were solubilized with Tris buffer. The OD values were measured at 560 nm

using a multi-well spectrophotometer (VERSA Max, Molecular Devices, Sunnyvale, CA). Average values determined from triplicate readings were used for the inhibitory rate calculation by the formula: $(OD_{control\ well} - OD_{treated\ well})/OD_{control\ well} - OD_{blank\ well} \times 100\%$. The IC_{50} was calculated using Logistic regression from three independent tests. Adriamycin was used as the positive control.

Immunosuppressive activity

Reagents: Concanavalin A (Con A), lipopolysaccharide (LPS, *Escherichia coli* 055:B5), CCK-8: WST-8 [2-(2-methoxy-4-nitrophenyl)-3-(4nitrophenyl)-5-(2, 4-disulfophenyl)-2H-tetrazolium, monosodium salt], and RPMI 1640 medium were purchased from GibcoBRL, Life Technologies (USA). Fetal bovine serum (FBS) was purchased from HyClone Laboratories (Utah, USA). [^{3}H]-Thymidine (10 μCi/mL) was obtained from the Shanghai Institute of Atomic Energy (SIAE).

Animals: Female BALB/C mice (7–9 weeks old) were obtained from Shanghai Experimental Animal Center and were housed in specific conditions (12 h light/12 h dark photoperiod, 22 ± 1 °C, 55% ± 5% relative humidity). All husbandry and experimental contact were made with the mice maintained specific pathogen-free conditions. All experiments were carried out according to the NIH Guidelines for Care and Use of Laboratory Animals and approved by the Bioethics Committee of Shanghai Institute of Materia Medica.

Preparation of spleen cells from mice: Female BALB/C mice were sacrificed by cervical dislocation, and the spleens were removed aseptically. Mononuclear cell suspensions were prepared after cell debris, and clumps were removed. Erythrocytes were depleted with ammonium chloride buffer solution. Lymphocytes were washed and resuspended in RPMI 1640 medium supplemented with 10% FBS, penicillin (100 U/mL), and streptomycin (100 mg/mL).

Cytotoxicity assay: Cytotoxicity was assessed with CCK-8 assay. Briefly, fresh spleen cells were obtained from female BALB/C mice (7–9 weeks old). Spleen cells (1×10^6 cells) were cultured at 37 ℃ for 48 h in 96-well flat plates, in the presence or absence of various concentrations of compounds, in a humidified and 5%

CO_2-containing incubator. A certain amount of CCK-8 was added to each well at the final 8–10 h of culture. To the end of the culture, we measured the OD values with microplate reader (Bio-Rad 650) at 450 nm. The cytotoxicity of each compound was expressed as the concentration of compound that reduced cell viability to 50% (CC_{50}).

T cell and B cell function assay: Fresh spleen cells were obtained from female BALB/C mice (7–9 weeks old). The 5×10^5 spleen cells were cultured at the same conditions as those mentioned above. The cultures, in the presence or absence of various concentrations of compounds, were stimulated with 5 μg/mL of ConA or 10 μg/mL of LPS to induce T cells or B cells proliferative responses, respectively. Proliferation was assessed in terms of uptake of [^{3}H]-thymidine during 8 h of pulsing with 25 μL/well of [^{3}H]-thymidine (10 μCi/mL), and then cells will be harvested onto glass fiber filters. The incorporated radioactivity was counted using a Beta scintillation counter (MicroBeta Trilux, PerkinElmer Life Sciences). The immunosuppressive activity of each compound was expressed as the concentration of compound that inhibited ConA-induced T cells proliferation or LPS-induced B cells proliferation to 50% (IC_{50}) of the control value.

NMR Calculation for Compound 1. In order to determine the specific structure and relative configuration of the lactone ring, four model compounds possessing all four possibilities of the lactone ring and without the triterpenoid side chain were designed (Figure 2). These model compounds were conformational analyzed via Monte Carlo searching using molecular mechanism with MMFF94 force field in the Spartan 08 program. [1] The result showed only one conformer for each of **1a**, **1b**, and **1d** and three conformers for **1c** whose relative energies within 2 Kcal/mol (Figure S5). These conformers were reoptimized using DFT at the B3LYP/6-31+G(d,p) level in vacuum using the Gaussian 09 program.[2] The B3LYP/6-31+G(d,p) harmonic vibrational frequencies were further calculated to confirm their stability. Gauge-Independent Atomic Orbital (GIAO) calculations of their ^{13}C-NMR chemical shifts were accomplished by density functional theory (DFT) at the rmpw1pw91/6-31+g(d,p) level. The calculated NMR data of the three lowest energy conformers of **1c** were averaged according to the Boltzmann distribution theory and their relative Gibbs free energy (ΔG). The ^{13}C-NMR chemical shifts for TMS were calculated by the same procedure and used as the reference.

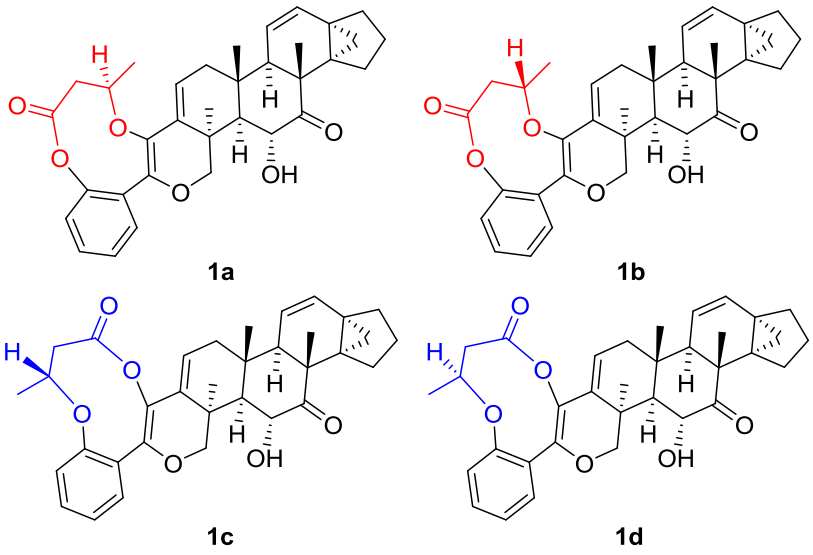

Figure 2. Four model compounds designed for the quantum chemical NMR calculation of compound **1**.

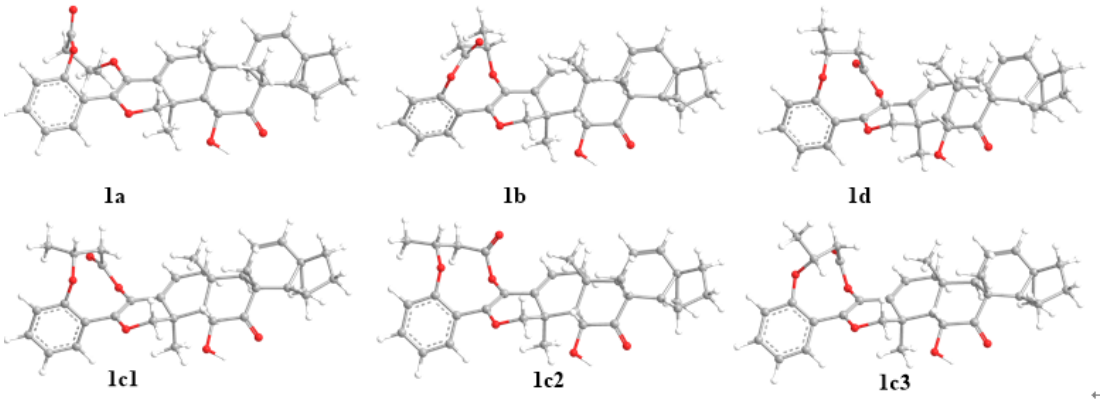

Figure S5. B3LYP/6-31+G(d,p) optimized lowest energy 3D conformers.

After calculation, chemical shifts of the lactone ring related carbons (C-1' – C-12') were selected for comparing with the experimental data. Linear correlation coefficients (R^2), root-mean-square deviation (RMSD) , and the DP4+ method[3] were adopted for evaluation of the results. The calculated data for **1a** showed the highest R^2 and lowest RMSD values among the calculated isomers (Table S3). A significant higher DP4+ probability score (95.89%) (Table S4) again suggested **1a** as the correct structure.

Energy analysis:

conf.	MMFF energy		b3lyp/6-311++g(2d,2p) Gibbs free energy (298.15 K)		
	ΔE (Kcal/mol)	Boltzmann. Distribution	G (Hartree)	ΔG (Kcal/mol)	Boltzmann Distribution
1c1	0.00	0.522	-1769.255699	1.332	0.095
1c2	0.27	0.332	-1769.252701	3.213	0.004
1c3	0.75	0.146	-1769.257822	0	0.901

Calculated NMR data:

Table S5. Calculated ^{13}C NMR chemical shifts.

No	Exp. data	**1a**	**1b**	**1c**	**1d**
1	40.5	43.78975	43.91585	43.87014	43.77405
2	112.9	123.739	120.0517	121.1693	120.1396
3	132.8	146.9633	145.6744	146.2398	145.3897
4	37.1	42.06205	43.14135	42.37094	42.45825

5	60.4	63.16275	63.61635	63.45904	63.88175
6	70.9	75.62455	75.97015	75.87241	75.63345
7	213.3	226.1925	226.7233	226.2957	225.8637
8	47.2	53.60175	53.58965	53.50474	53.88055
9	51.6	55.24935	56.34505	56.34722	55.93725
10	37.3	43.86295	41.57075	41.89943	42.54515
11	120.3	126.9416	127.355	126.5429	127.4313
12	131.8	144.6643	142.8375	143.3688	143.5656
13	31.7	36.20195	38.92645	39.03992	37.34865
14	36.6	43.80725	44.00595	43.15212	43.36165
15	26.8	31.61845	32.14635	31.92317	31.61655
16	23.8	25.32515	26.86675	26.99452	26.02005
17	40.7	34.78795	34.91915	34.54882	34.19425
18	17.3	18.89575	19.07955	19.14302	18.74355
19	16.4	17.40495	17.27205	17.49636	17.21035
28	28.1	29.19635	29.04675	28.98609	28.68855
29	72.7	72.82635	73.06125	73.18243	73.63985
30	14.5	18.67995	19.16325	18.71542	18.16935
1′	137.1	145.8532	143.0048	135.2197	136.7996
2′	136.7	142.9734	151.3554	152.1989	153.9867
3′	121.4	137.0203	136.7524	128.1573	135.0515
4′	118.3	136.3198	138.0437	136.6565	136.4768
5′	122.7	131.3691	130.3412	126.7607	129.6947
6′	124.9	134.2569	135.8272	135.8431	137.677
7′	111.6	128.2719	125.6428	127.0245	128.5756
8′	153.3	155.9307	158.8269	164.0677	166.1371
9′	173.7	174.9677	176.9105	177.5801	178.5274
10′	43.4	46.92565	43.67835	46.33089	43.70025
11′	64.5	76.89055	83.00425	78.1777	86.65625
12′	22.8	23.87665	23.26725	23.88199	25.00775

References and Notes

1. Spartan 04; Wavefunction Inc.: Irvine, CA.

2. Gaussian 09, Rev. C 01. Frisch, M. J.; Trucks, G. W.; Schlegel, H. B.; Scuseria, G. E.; Robb, M. A.; Cheeseman, J. R.; Scalmani, G.; Barone, V.; Mennucci, B.; Petersson, G. A.; Nakatsuji, H.; Caricato, M.; Li, X.; Hratchian, H. P.; Izmaylov, A. F.; Bloino, J.; Zheng, G.; Sonnenberg, J. L.; Hada, M.; Ehara, M.; Toyota, K.; Fukuda, R.; Hasegawa, J.; Ishida, M.; Nakajima, T.; Honda, Y.; Kitao, O.; Nakai, H.; Vreven,

T.; Montgomery, Jr., J. A.; Peralta, J. E.; Ogliaro, F.; Bearpark, M.; Heyd, J. J.; Brothers, E.; Kudin, K. N.; Staroverov, V. N.; Kobayashi, R.; Normand, J.; Raghavachari, K.; Rendell, A.; Burant, J. C.; Iyengar, S. S.; Tomasi, J.; Cossi, M.; Rega, N.; Millam, J. M.; Klene, M.; Knox, J. E.; Cross, J. B.; Bakken, V.; Adamo, C.; Jaramillo, J.; Gomperts, R.; Stratmann, R. E.; Yazyev, O.; Austin, A. J.; Cammi, R.; Pomelli, C.; Ochterski, J. W.; Martin, R. L.; Morokuma, K.; Zakrzewski, V. G.; Voth, G. A.; Salvador, P.; Dannenberg, J. J.; Dapprich, S.; Daniels, A. D.; Farkas, Ö.; Foresman, J. B.; Ortiz, J. V.; Cioslowski, J.; Fox, D. J. Gaussian, Inc., Wallingford CT, 2009.

3. Grimblat, N.; Zanardi, M. M.; Sarotti, A. M. *J. Org. Chem.* **2015**, *80*, 12526-12534.

The NMR data analogy of compound 1 with model compounds.

The formation of an ester at the C-8′ of **1** was further corroborated by comparing its C-8′ chemical shift with those of the key carbons in the model compounds **1e**[4] and **1f**[5] (Figure S6), in which the chemical shift of C-8′ at 153.3 of **1** is more close to that (δ_C150.8) of model **1e**. If it had an ether bond between C-8′ and C-9′, the C-8′(153.3 ppm) of **1** would be more deshielded than the key carbon (159.0 ppm) of **1f** due to the more deshielding chemical environments around the C-8′ of **1**.

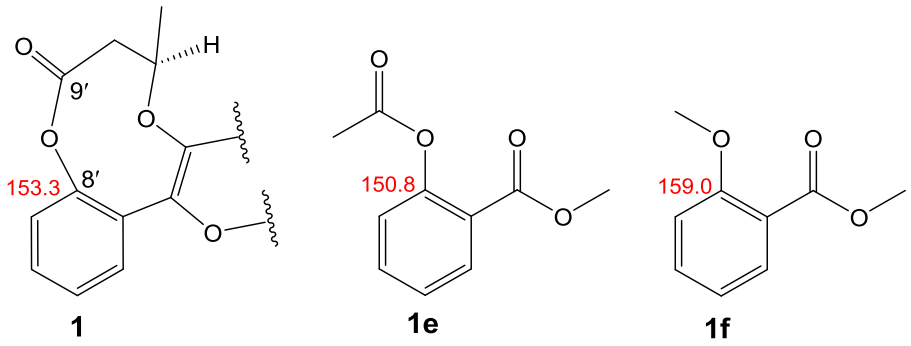

Figure S6. The key chemical shift of **1** and those of model compounds **1e** and **1f** (all measured in $CDCl_3$).

References

4. Liu, Y. Y.; Qi, J. M.; Bai, L. S.; Xu, Y. L.; Ma, N.; Sun, F. F. *Chin. Chem. Lett.* **2016**, *27*, 726-730.

5. Li, P.; Zhao, J. J.; Lang, R.; Li, F. W. *Tetrahedron Lett.* **2014**, *55*, 390 –393.

ECD Calculation for Compound 1. The absolute configuration of compound **1** was determined by comparing the experimental ECD spectrum with quantum chemical TDDFT calculated theoretical ECD spectrum of the model compound **1a**. The B3LYP/6-31+G(d,p) optimized geometry in the NMR calculation was adopted for further computation. The energies, oscillator strengths, and rotational strengths of the first 60 electronic excitations were calculated using the TDDFT methodology at the B3LYP/6-311++G(2d,2p) level in vacuum. The ECD spectrum were simulated by the overlapping Gaussian function (σ = 0.6 eV),[6] in which velocity rotatory strengths of the first 40 exited states were adopted.

In the 150-450 nm region (Figure 4), both the experimental and predicted ECD spectra showed first and second positive Cotton effects around 325 and 250 nm, and a third negative Cotton effect around 210 nm. Therefore, qualitative analysis of the predicted and experimental ECD spectra allowed the assignments of the absolute configuration of compound **1**.

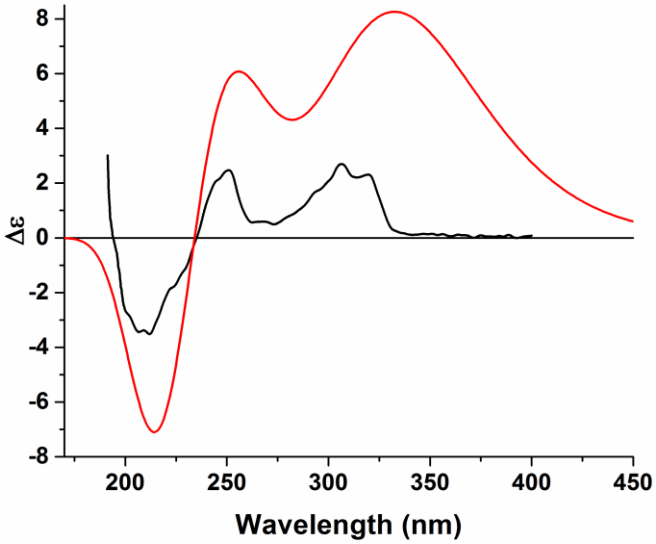

Figure 4. Experimental CD spectrum of compound **1** (black line) and calculated ECD spectrum of model compound **1a** (red line).

ECD simulation:

ECD spectrum of each conformation is simulated according to the overlapping Gaussian functions expressed as:

$$\Delta\varepsilon(E)=\frac{1}{2.296\times10^{-39}\sqrt{\pi}\sigma}\sum_{i}^{A}\Delta E_i R_i e^{[-(E-\Delta Ei)^2/\sigma^2]}$$

Where σ is half the bandwidth at 1/e peak height and expressed in energy units. The parameters ΔE_i and R_i are the excitation energies and rotational strengths for the transition *i*, respectively.

The above function is converted to Δε, λ (wavelength) correlations as:

$$\Delta\varepsilon(\lambda)=\frac{1}{2.296\times10^{-39}\sqrt{\pi}\sigma}\sum_{i}^{A}\Delta E_i R_i e^{[-(1240/\lambda-\Delta Ei)^2/\sigma^2]}$$

and then simulation were accomplished by using the Excel 2003 and the Origin 7.0 software.

To get the final spectra, all the simulated spectra of conformations of each compound were averaged according to their energy and the Boltzmann distribution theory expressed as:

$$\frac{N_i^*}{N}=\frac{g_i e^{-\varepsilon_i/k_B T}}{\sum g_i e^{-\varepsilon_i/k_B T}}$$

Calculated ECD Data：

State	**C1**	
	Excitation energies(eV)	Rotatory Strengths*
1	3.7147	49.131
2	3.879	1.7854
3	4.0347	7.6697
4	4.3784	-11.344
5	4.5004	6.0155
6	4.5899	-2.3222
7	4.6278	-4.5194
8	4.6807	0.0522
9	4.7488	-1.4255
10	4.7889	3.2677
11	4.869	-0.152
12	4.9542	-6.0769

13	4.9671	32.3218
14	5.1009	-0.7893
15	5.1229	11.3898
16	5.1402	17.0172
17	5.1941	5.9966
18	5.3202	0.2926
19	5.3577	33.3483
20	5.3723	-62.0494
21	5.3931	-6.5887
22	5.4171	-0.8838
23	5.4887	8.9872
24	5.4921	15.7828
25	5.5027	-5.8675
26	5.5127	-7.3124
27	5.5167	-16.8189
28	5.5454	2.7086
29	5.5531	0.2825
30	5.5776	1.2251
31	5.6131	-4.5025
32	5.6628	-1.5006
33	5.6738	-0.9458
34	5.6802	5.9273
35	5.7074	-0.7577
36	5.7236	-2.0425
37	5.7331	1.1068
38	5.8003	-4.4273
39	5.8122	-19.3866
40	5.8395	6.1074
41	5.8399	-0.2306
42	5.8421	-7.3568
43	5.8877	-4.1287
44	5.8953	-17.8094
45	5.9325	1.8982
46	5.9416	5.1326
47	5.9491	-9.5241
48	5.9547	-2.0005
49	6.0183	-4.5707
50	6.0297	-2.0942
51	6.0326	0.5544
52	6.0845	18.0536
53	6.0911	-9.8168
54	6.1016	3.1388
55	6.1122	6.7369

56	6.1466	-4.3245
57	6.1566	1.4889
58	6.166	2.1568
59	6.1749	-0.3546
60	6.1778	-18.5752

* R(velocity) 10**-40 erg-esu-cm

References and Notes

6. Stephens, P. J.; Harada, N. ECD cotton effect approximated by the Gaussian curve and other methods. *Chirality* **2010**, *22*, 229–233.

Figure S7. ^{1}H NMR spectrum of phainanolide A (**1**) in $CDCl_3$

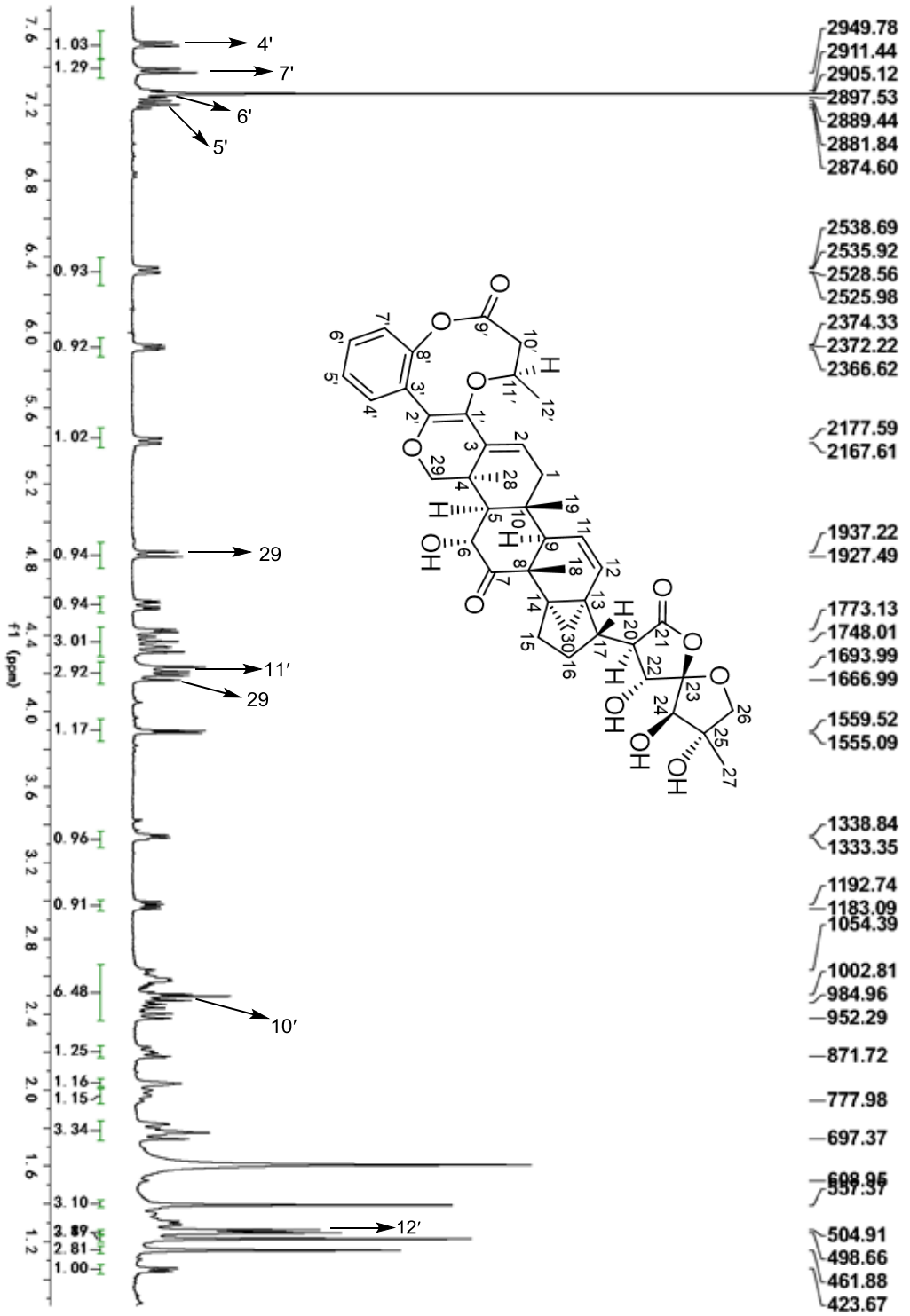

Figure S8. ^{13}C NMR spectrum of phainanolide A (**1**) in $CDCl_3$

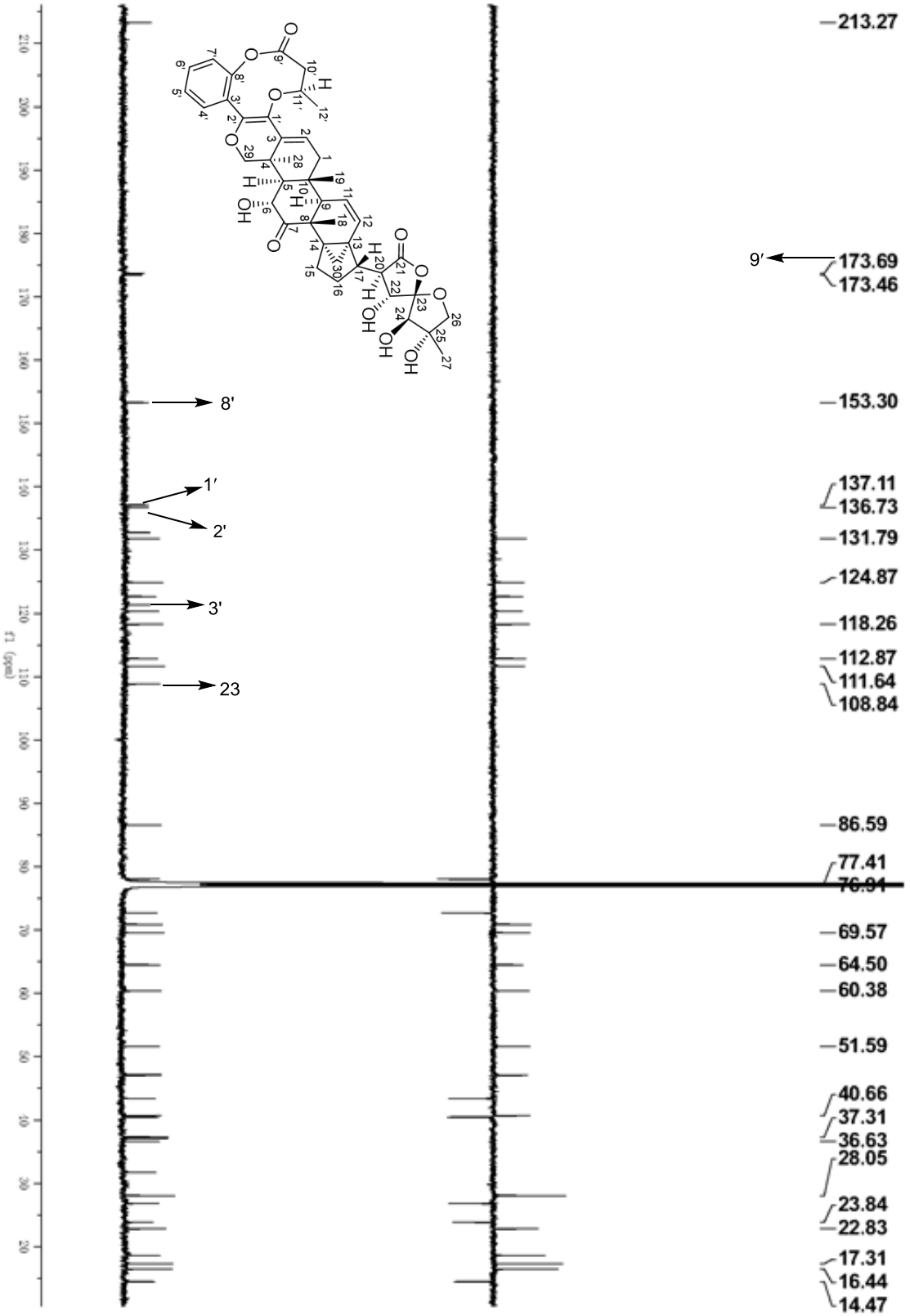

Figure S9. HSQC spectrum of phainanolide A (**1**) in $CDCl_3$

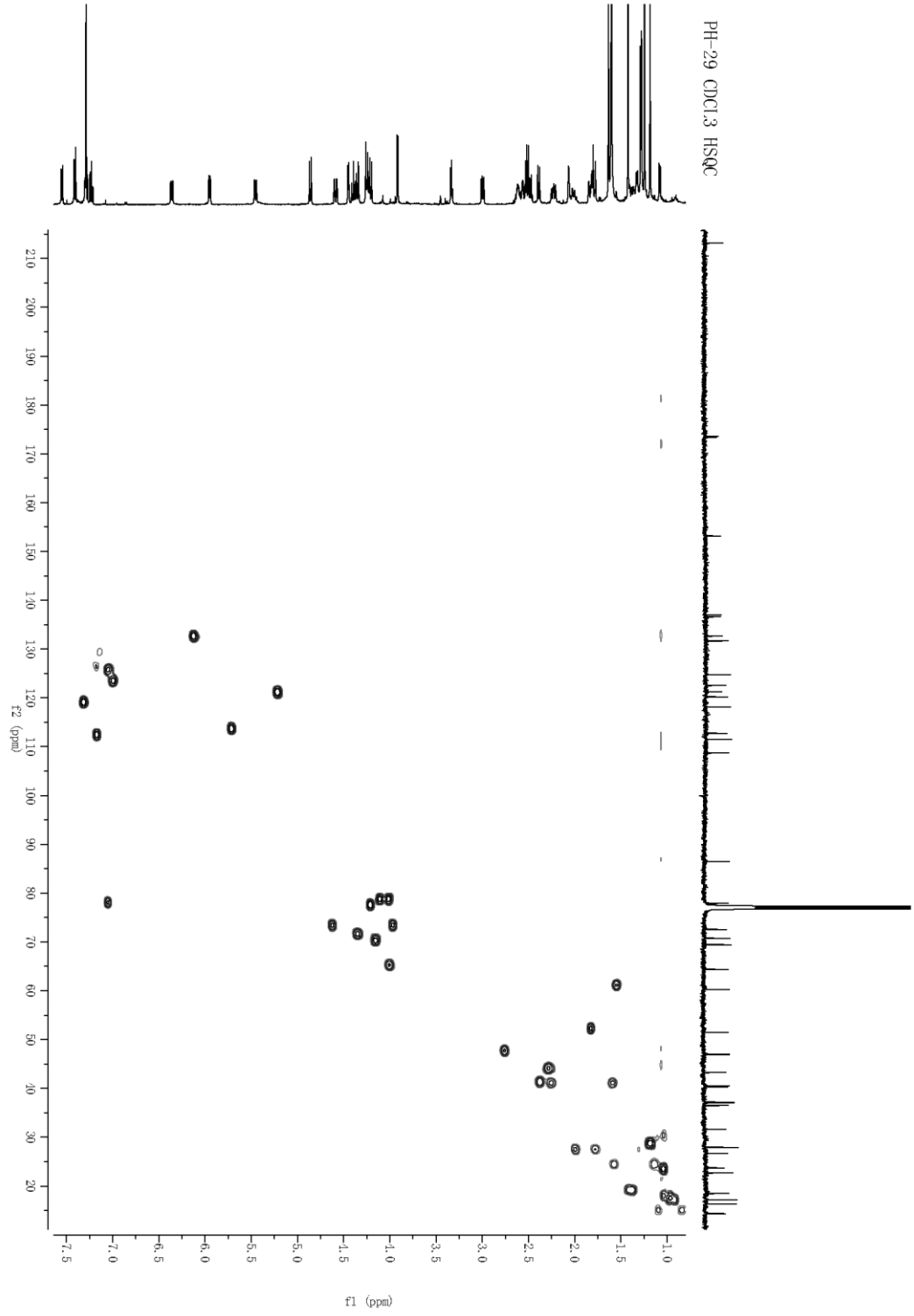

Figure S10. HMBC spectrum of phainanolide A (**1**) in $CDCl_3$

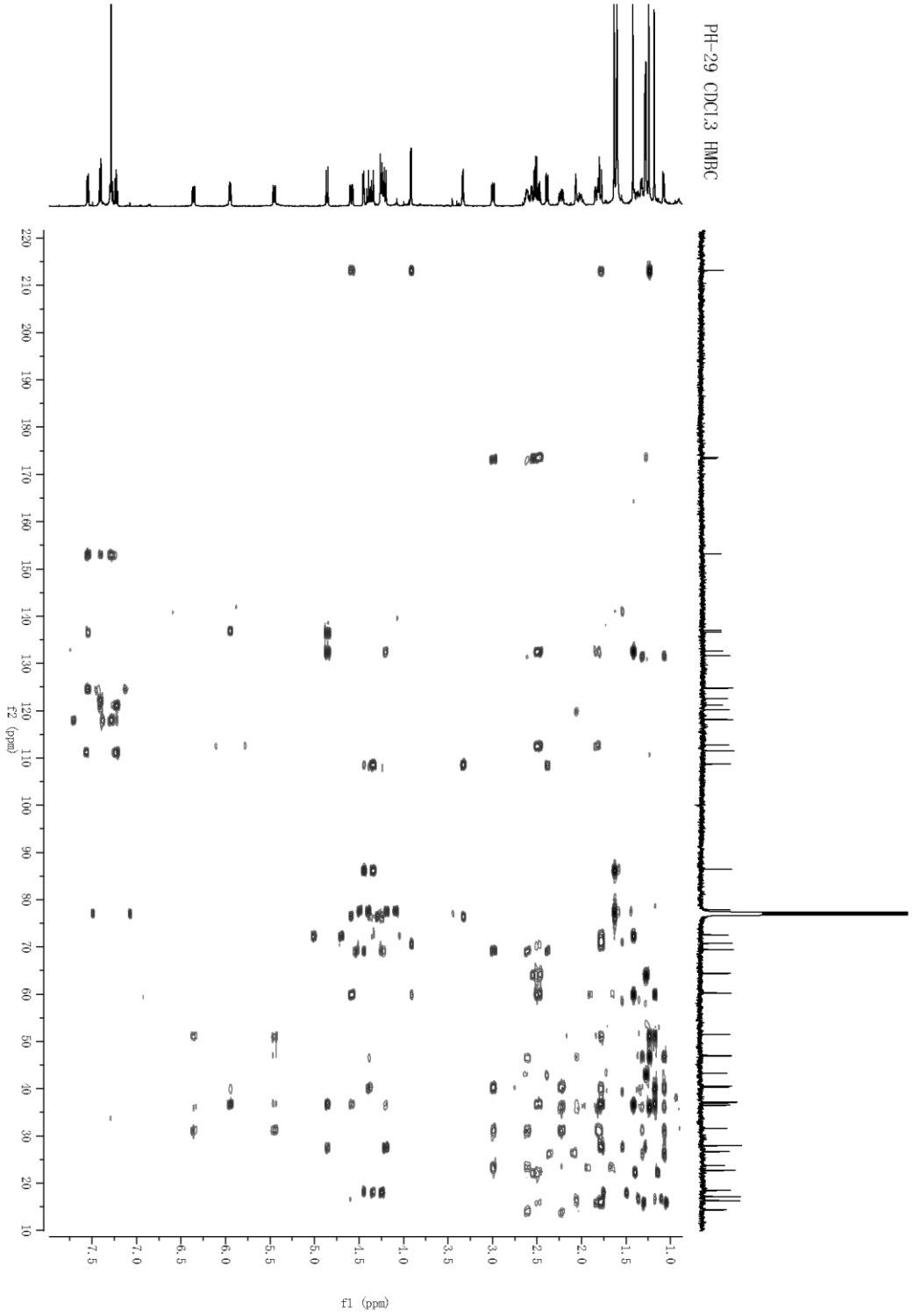

Figure S11. $^{1}H–^{1}H$ COSY spectrum of phainanolide A (**1**) in $CDCl_3$

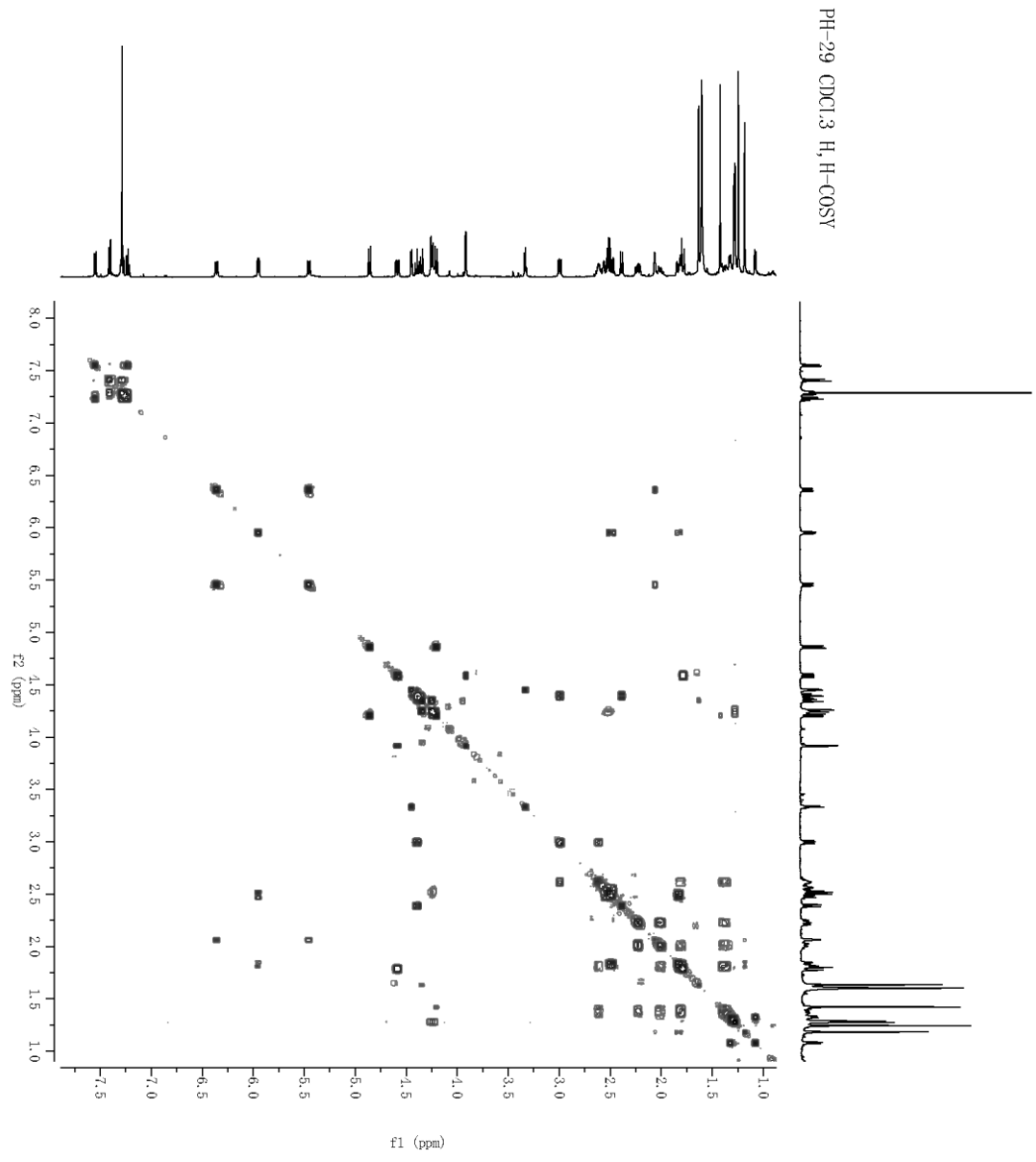

Figure S12. NOESY spectrum of phainanolide A (**1**) in $CDCl_3$

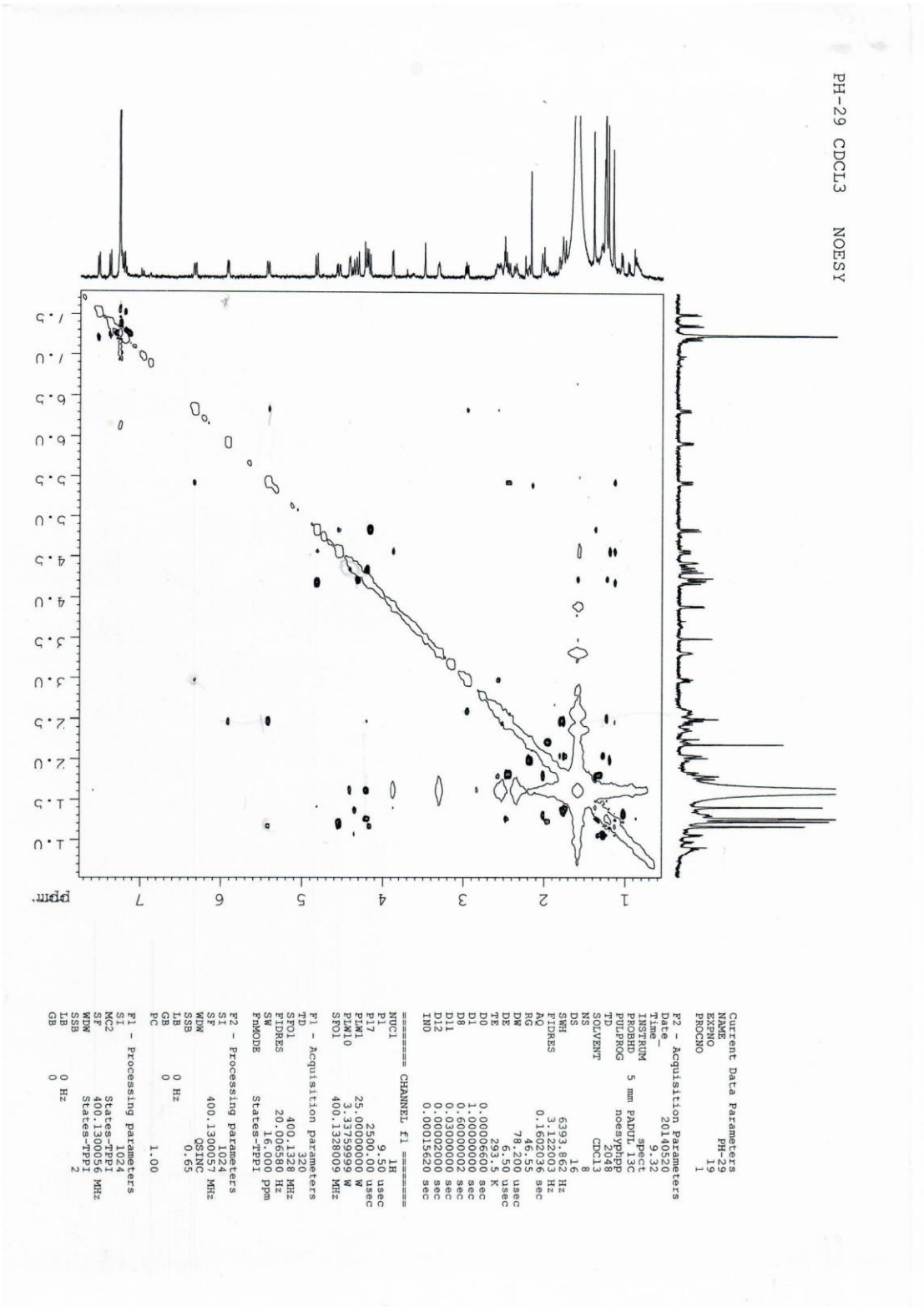

Figure S13. ESI(+)MS spectrum of phainanolide A (**1**)

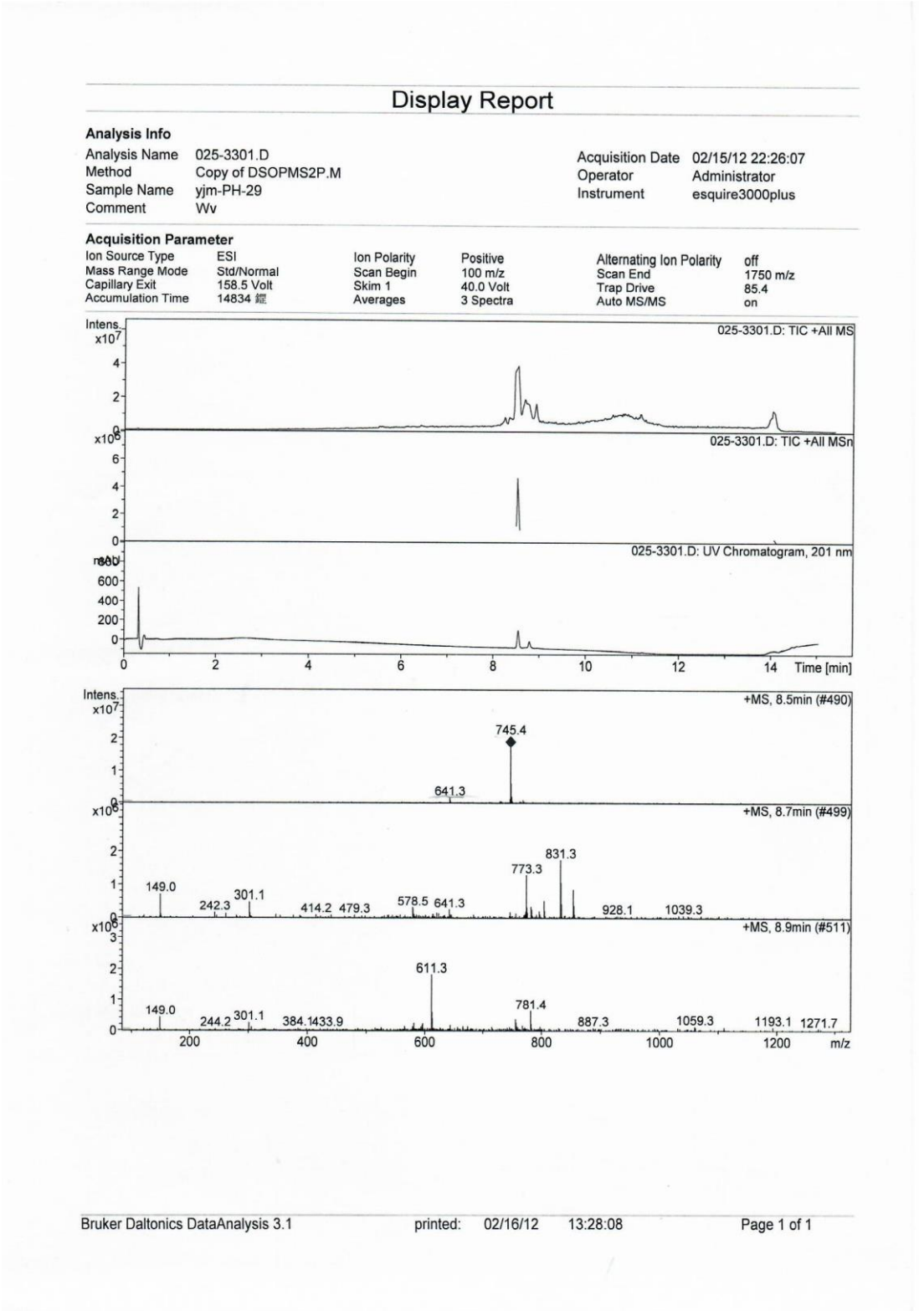

Figure S14. ESI(–)MS spectrum of phainanolide A (**1**)

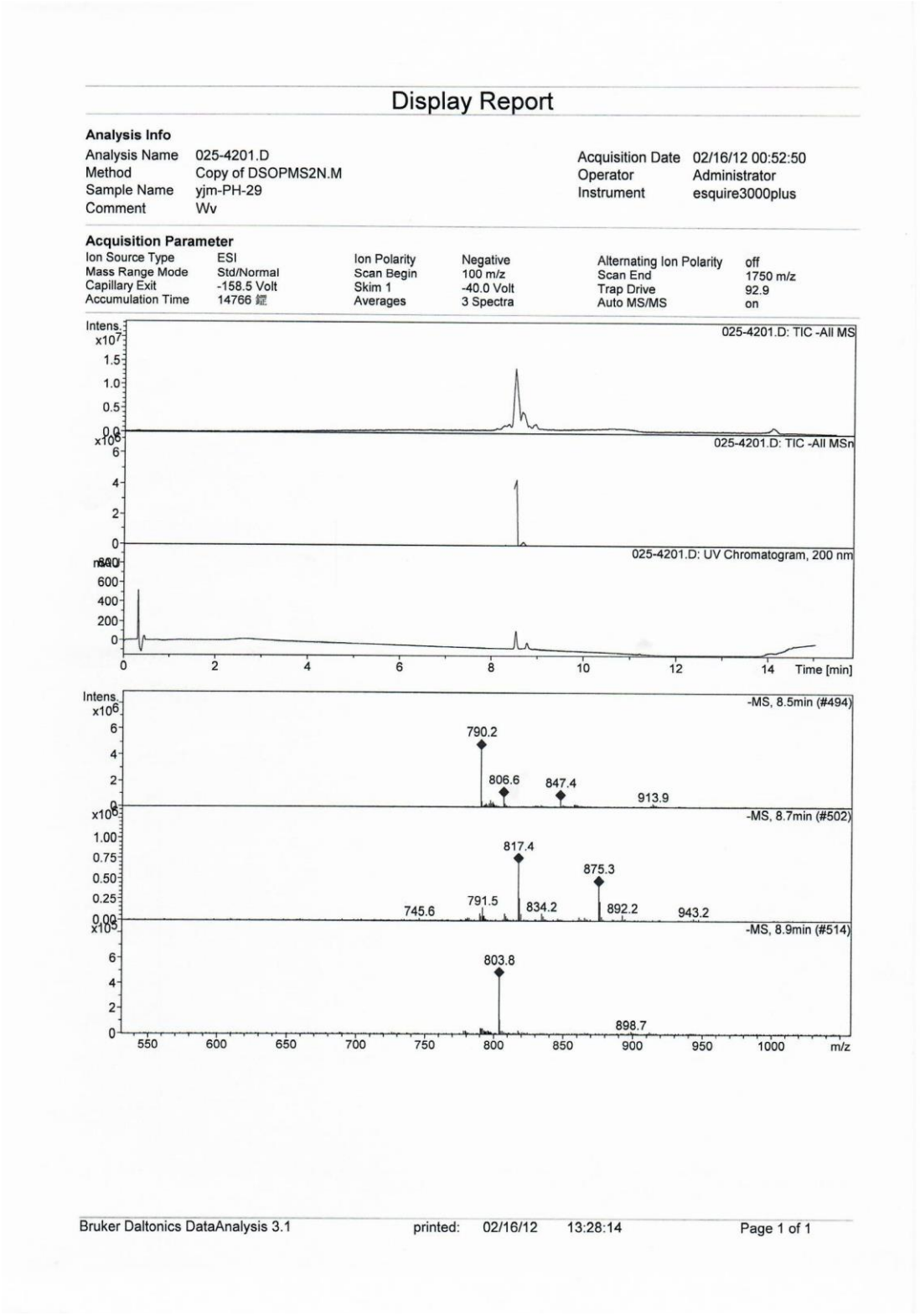

Figure S15. HRESI(–)MS spectrum of phainanolide A (**1**)

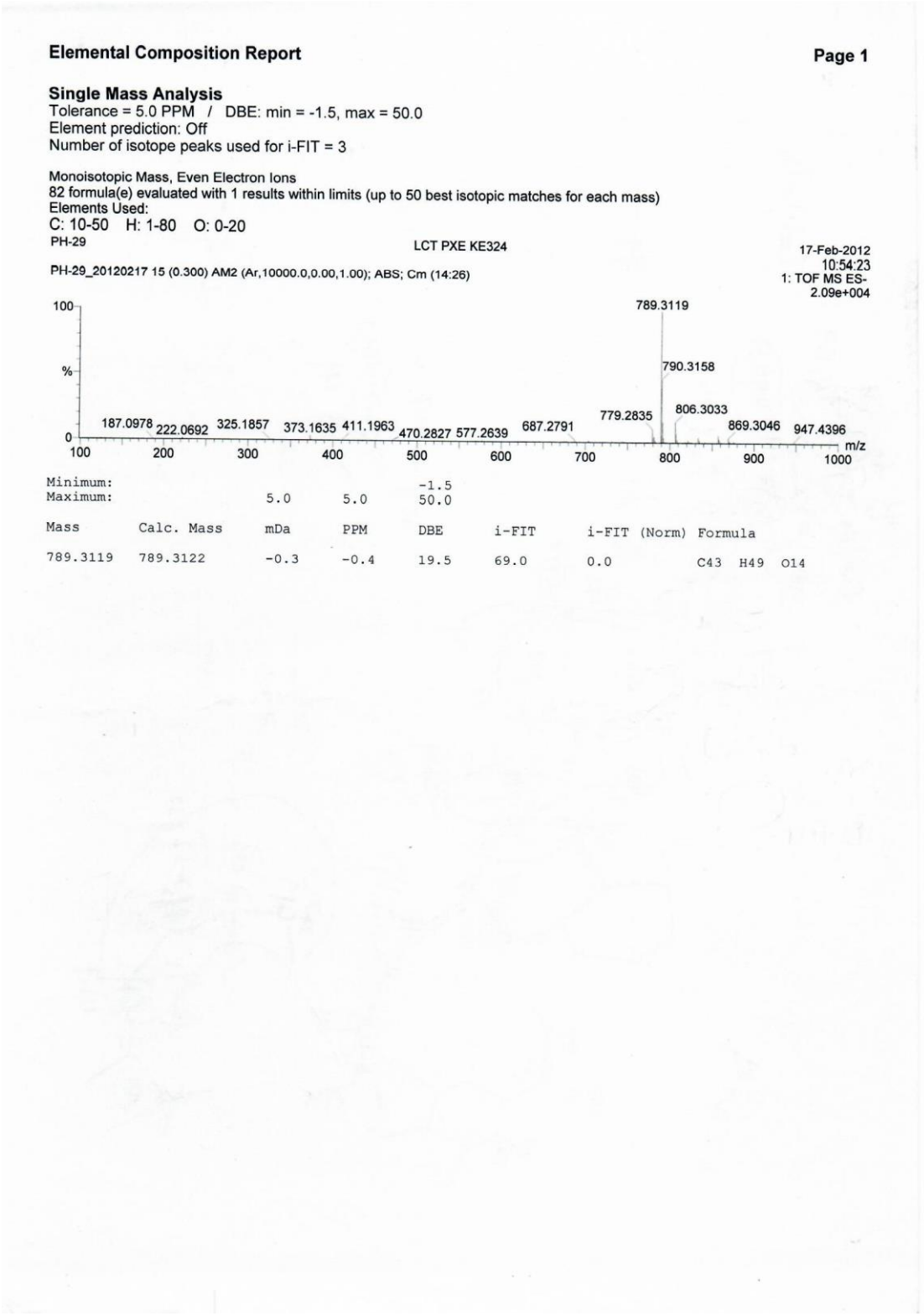

Elemental Composition Report **Page 1**

Single Mass Analysis
Tolerance = 5.0 PPM / DBE: min = -1.5, max = 50.0
Element prediction: Off
Number of isotope peaks used for i-FIT = 3

Monoisotopic Mass, Even Electron Ions
82 formula(e) evaluated with 1 results within limits (up to 50 best isotopic matches for each mass)
Elements Used:
C: 10-50 H: 1-80 O: 0-20

PH-29 LCT PXE KE324 17-Feb-2012 10:54:23

PH-29_20120217 15 (0.300) AM2 (Ar,10000.0,0.00,1.00); ABS; Cm (14:26) 1: TOF MS ES- 2.09e+004

Minimum:				-1.5			
Maximum:		5.0	5.0	50.0			
Mass	Calc. Mass	mDa	PPM	DBE	i-FIT	i-FIT (Norm)	Formula
789.3119	789.3122	-0.3	-0.4	19.5	69.0	0.0	C43 H49 O14

Figure S16. IR spectrum of phainanolide A (**1**)

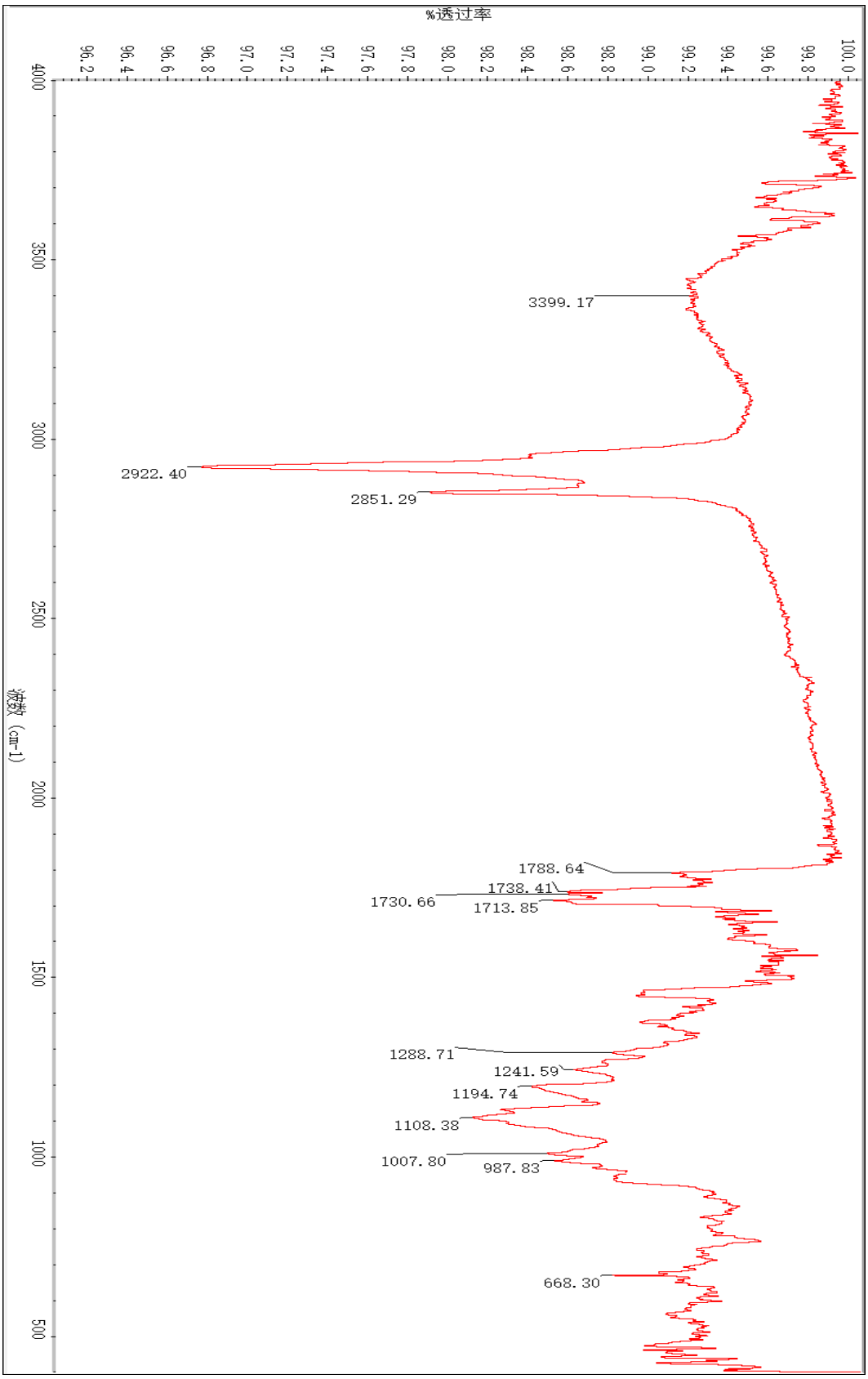

Figure S17. ^{1}H NMR spectrum of phainanoid G (**2**) in $CDCl_3$

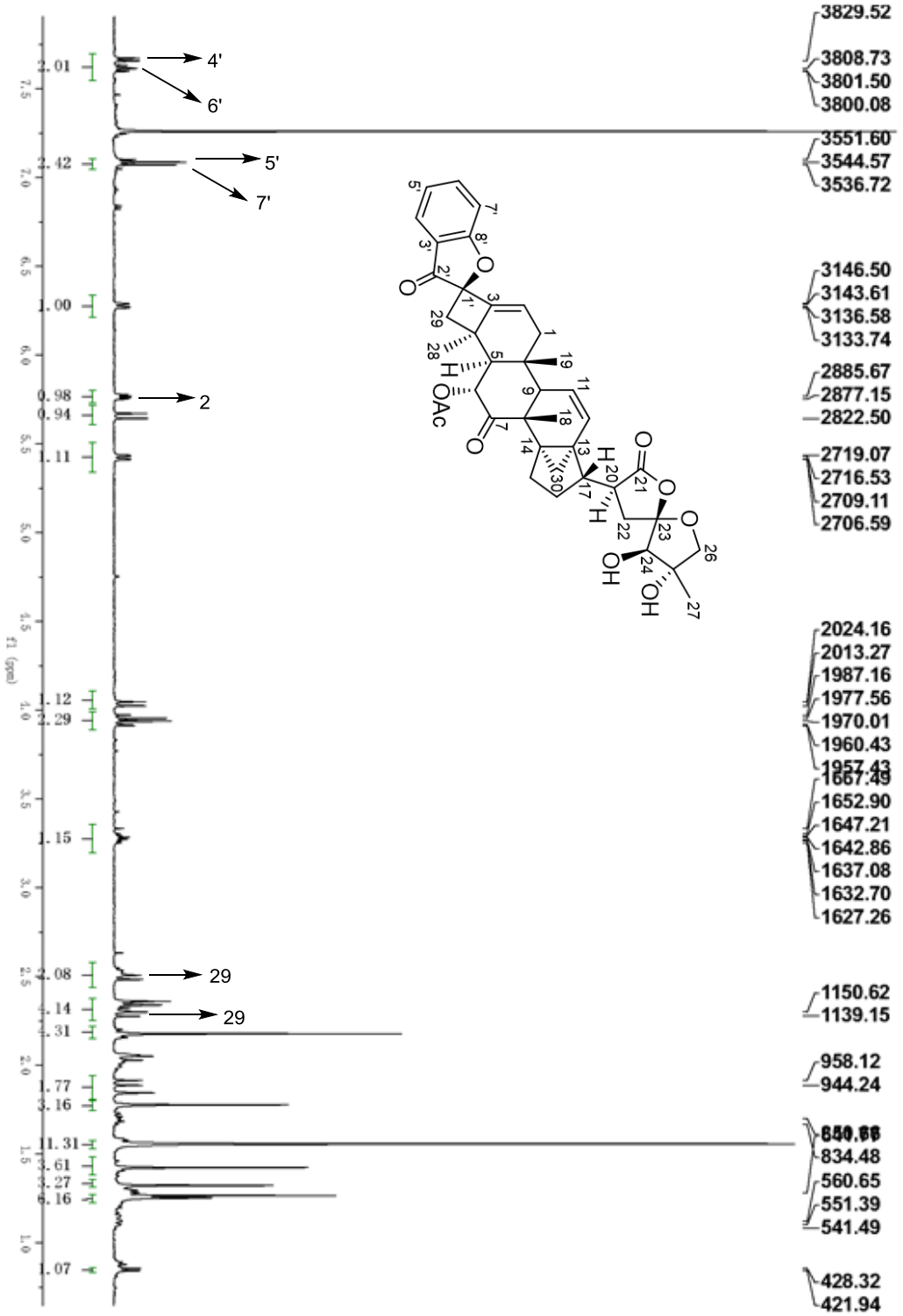

Figure S18. ^{13}C NMR spectrum of phainanoid G (**2**) in $CDCl_3$

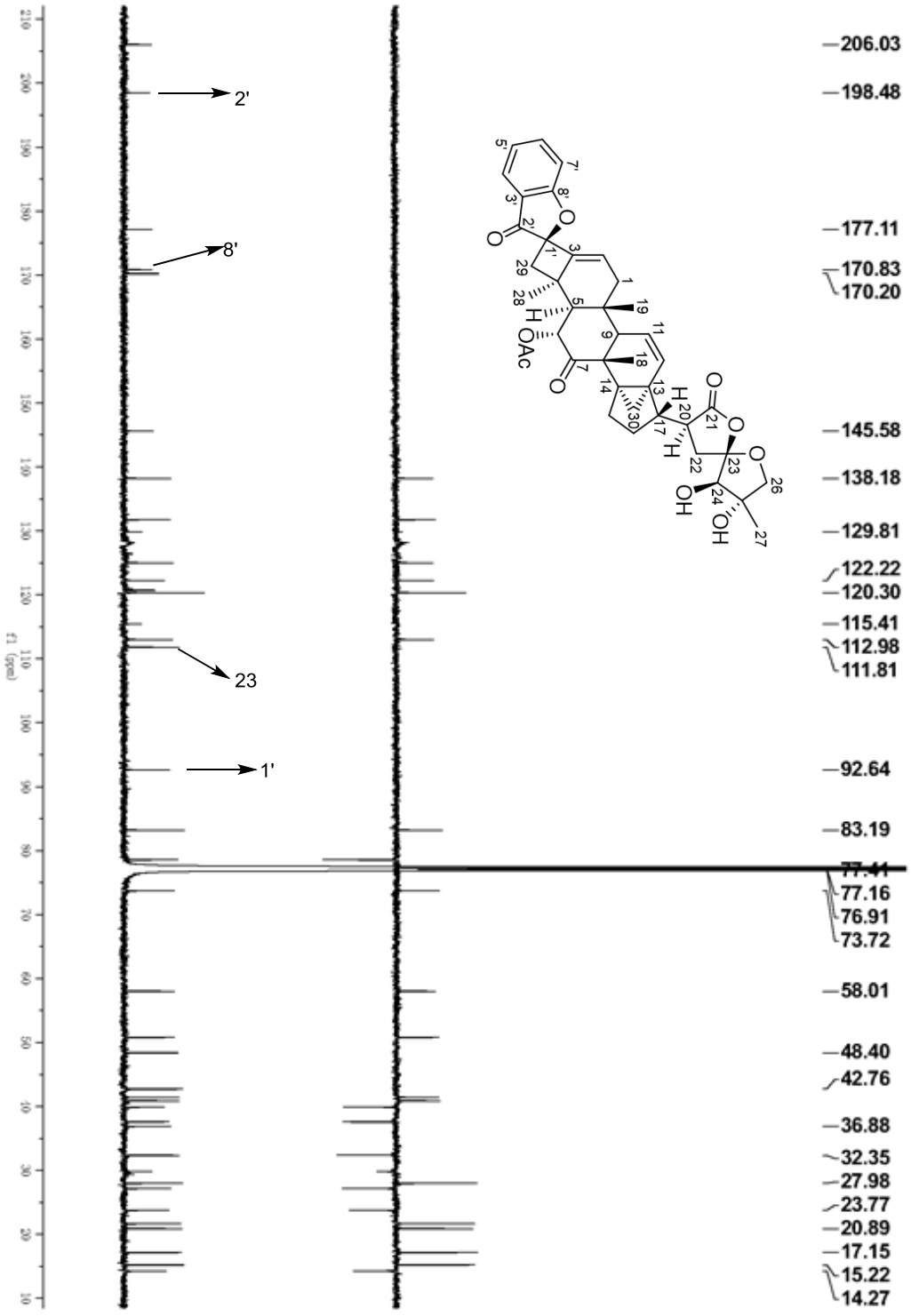

Figure S19. HSQC spectrum of phainanoid G (**2**) in $CDCl_3$

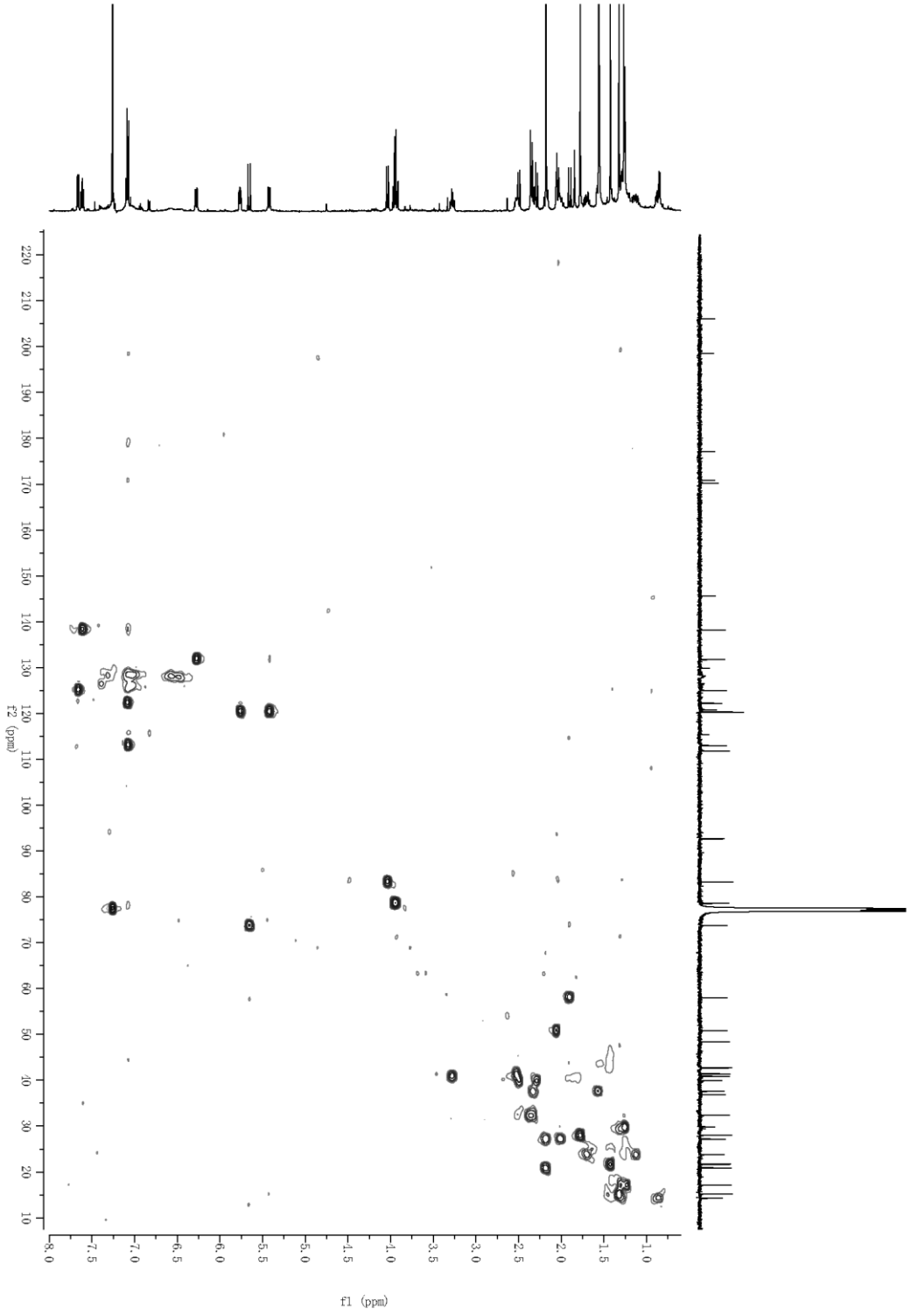

Figure S20. HMBC spectrum of phainanoid G (**2**) in $CDCl_3$

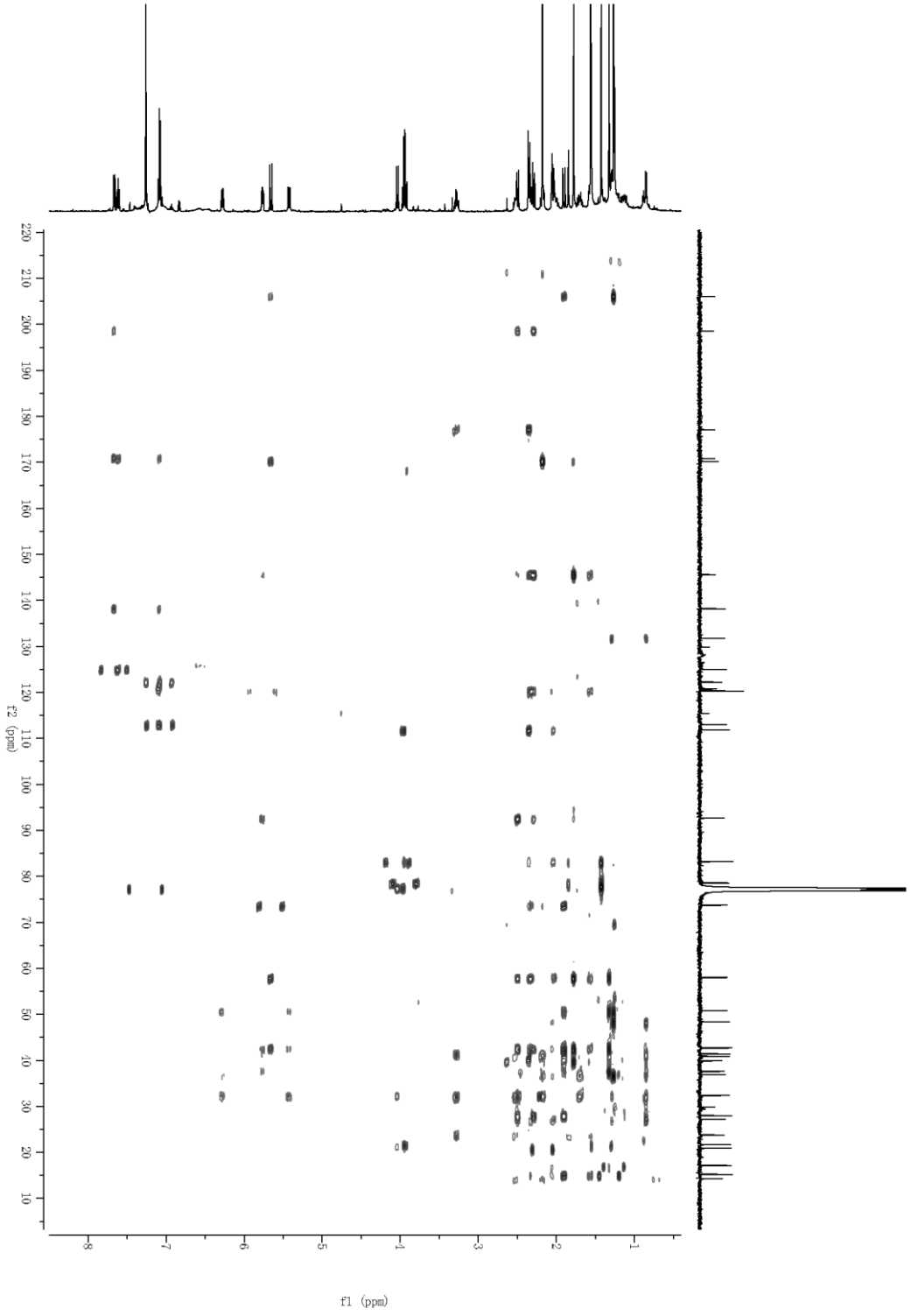

Figure S21. $^{1}H–^{1}H$ COSY spectrum of phainanoid G (**2**) in $CDCl_3$

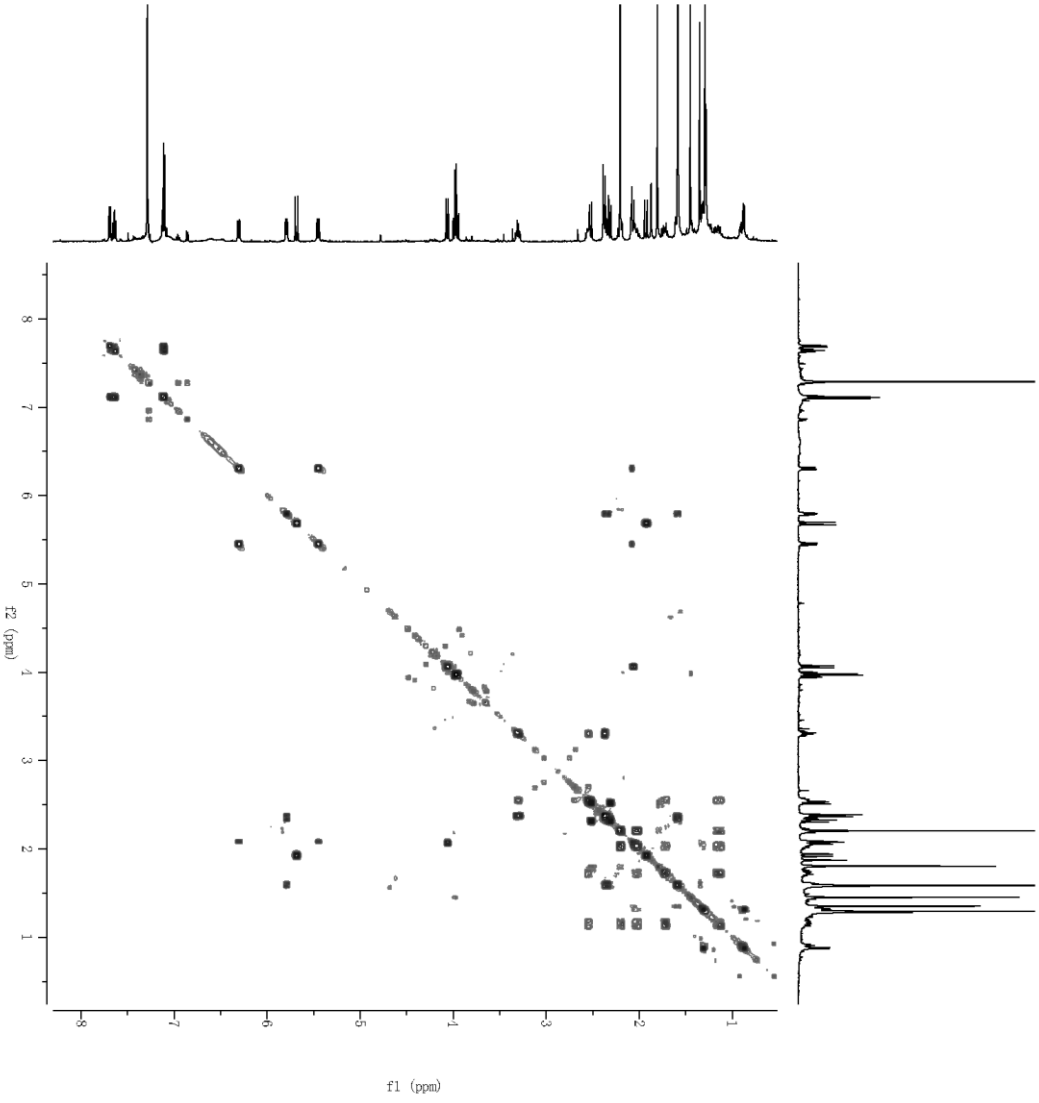

Figure S22. ROESY spectrum of phainanoid G (**2**) in $CDCl_3$

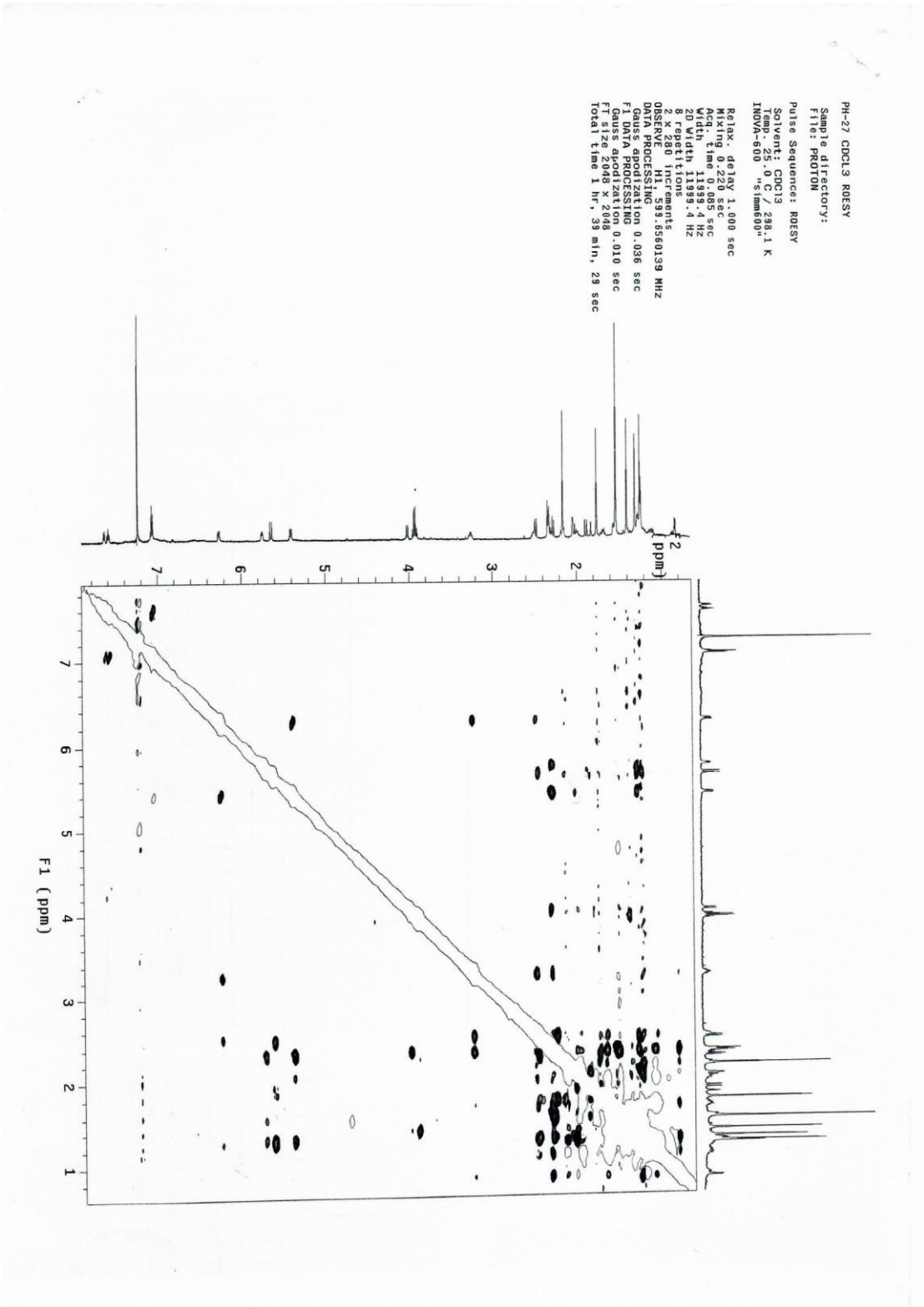

Figure S23. ESI(+)MS spectrum of phainanoid G (**2**)

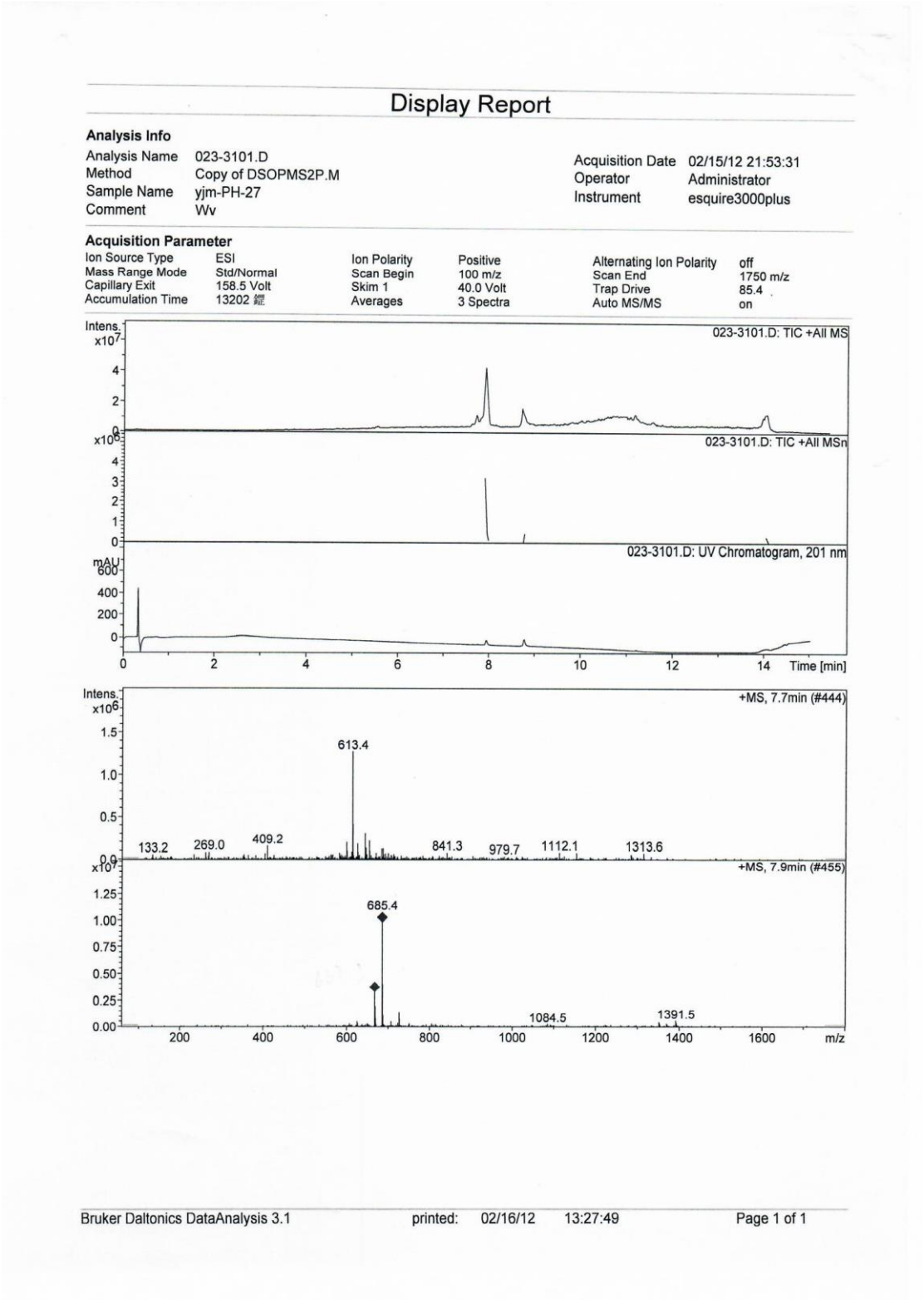

Figure S24. ESI(–)MS spectrum of phainanoid G (**2**)

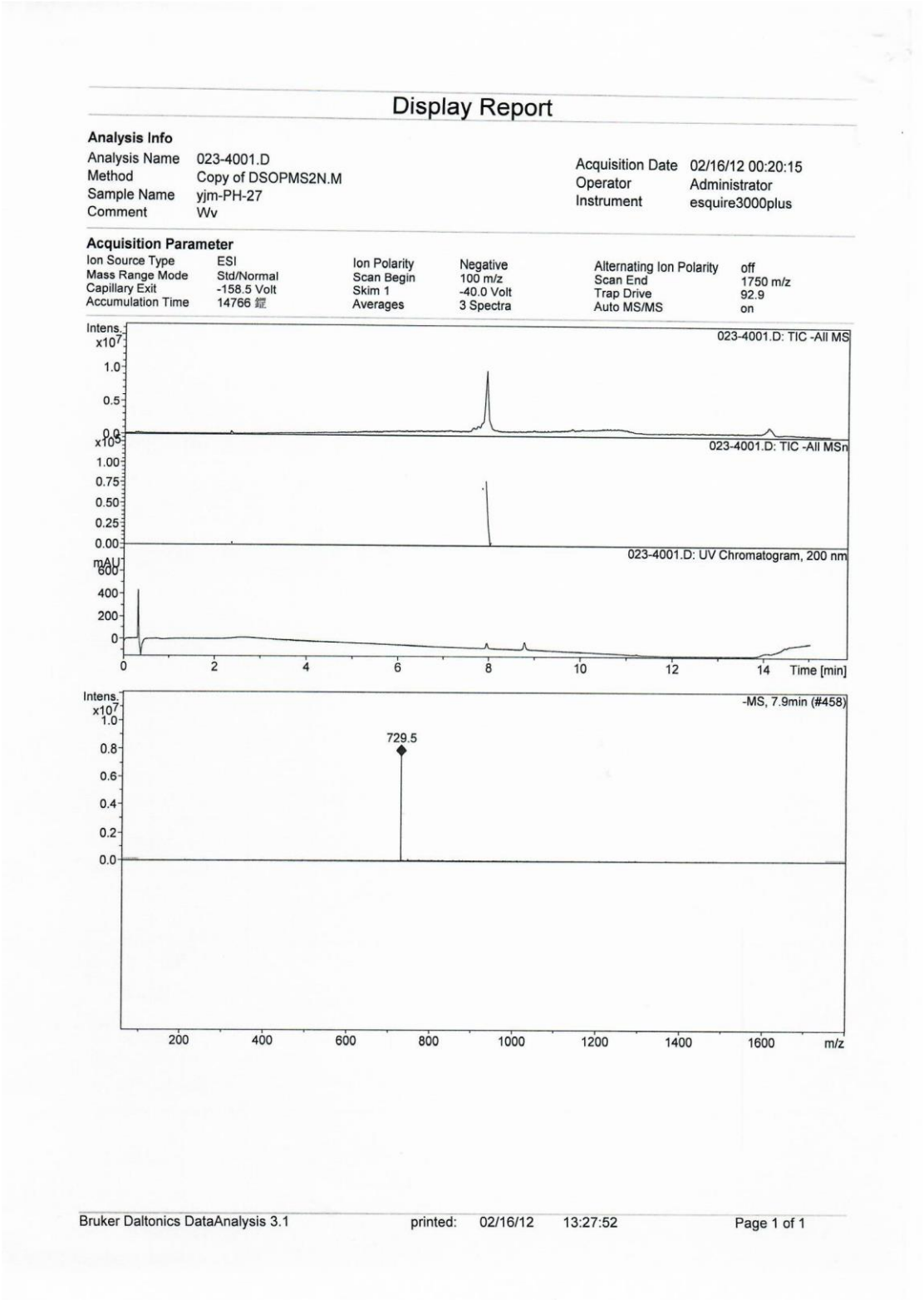

Figure S25. HRESI(–)MS spectrum of phainanoid G (**2**)

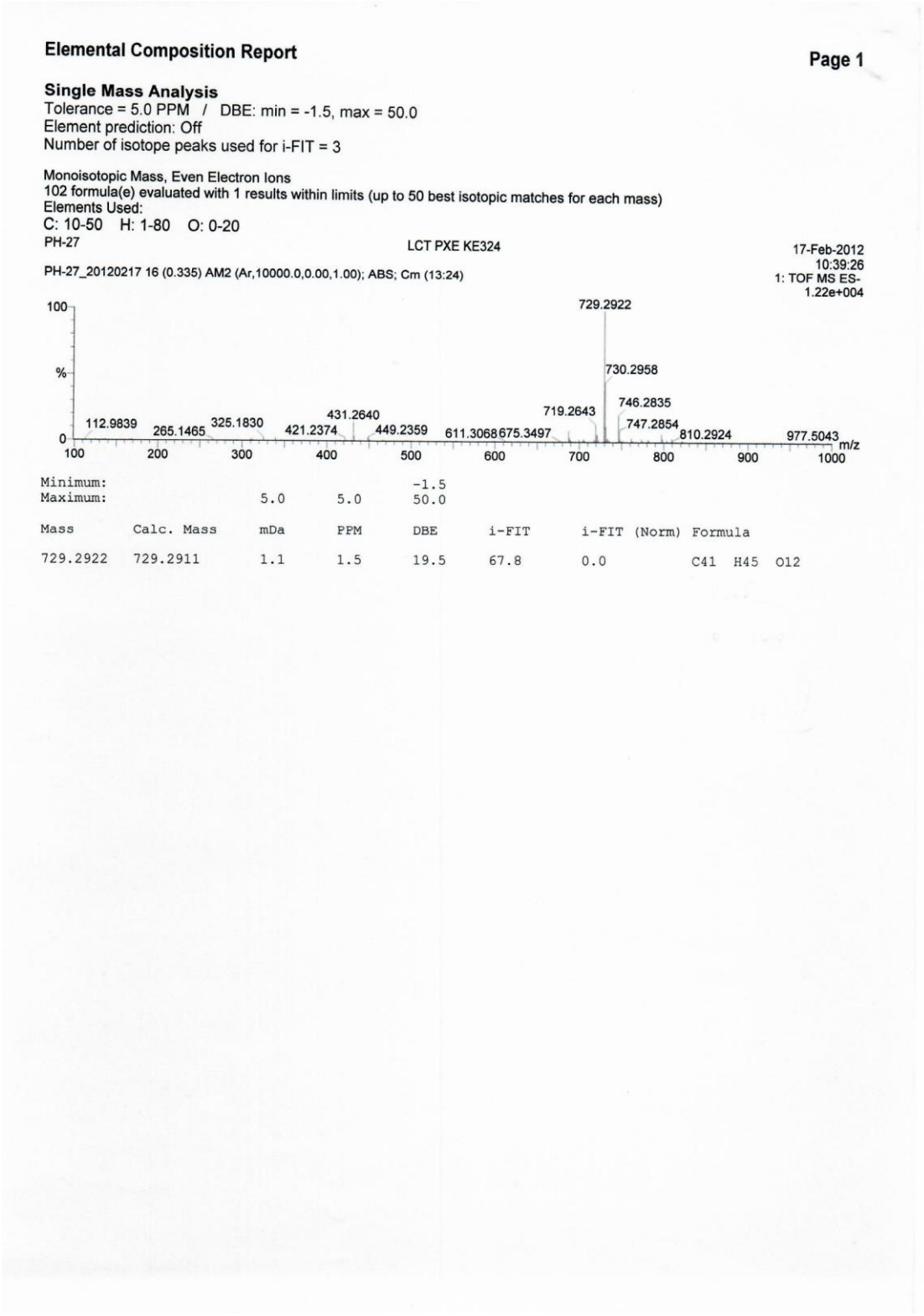

Elemental Composition Report Page 1

Single Mass Analysis
Tolerance = 5.0 PPM / DBE: min = -1.5, max = 50.0
Element prediction: Off
Number of isotope peaks used for i-FIT = 3

Monoisotopic Mass, Even Electron Ions
102 formula(e) evaluated with 1 results within limits (up to 50 best isotopic matches for each mass)
Elements Used:
C: 10-50 H: 1-80 O: 0-20

PH-27 LCT PXE KE324 17-Feb-2012 10:39:26

PH-27_20120217 16 (0.335) AM2 (Ar,10000.0,0.00,1.00); ABS; Cm (13:24) 1: TOF MS ES- 1.22e+004

Minimum:				-1.5			
Maximum:		5.0	5.0	50.0			
Mass	Calc. Mass	mDa	PPM	DBE	i-FIT	i-FIT (Norm)	Formula
729.2922	729.2911	1.1	1.5	19.5	67.8	0.0	C41 H45 O12

Figure S26. IR spectrum of phainanoid G (**2**)

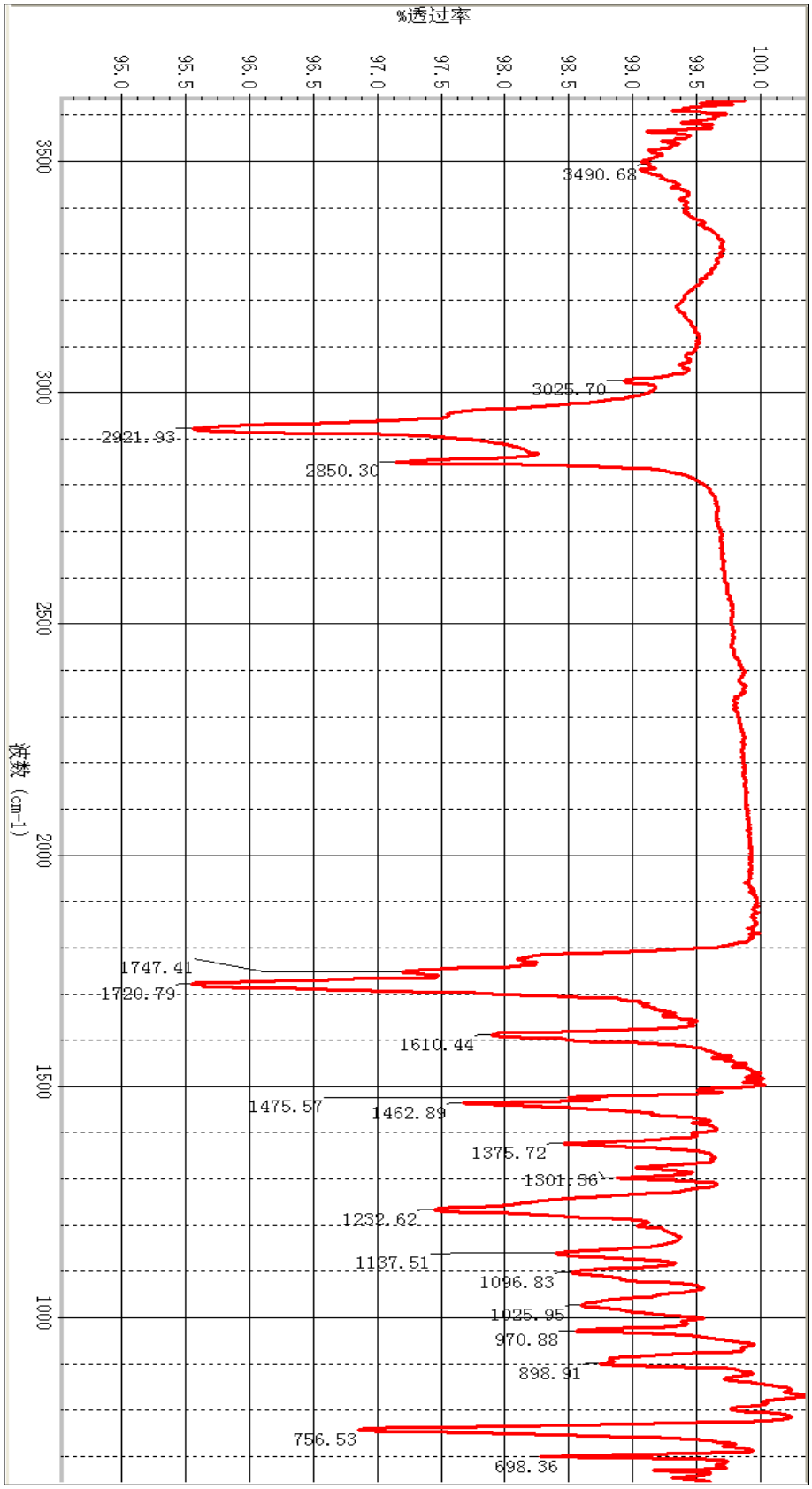

Figure S27. ^{1}H NMR spectrum of phainanoid H (**3**) in $CDCl_3$

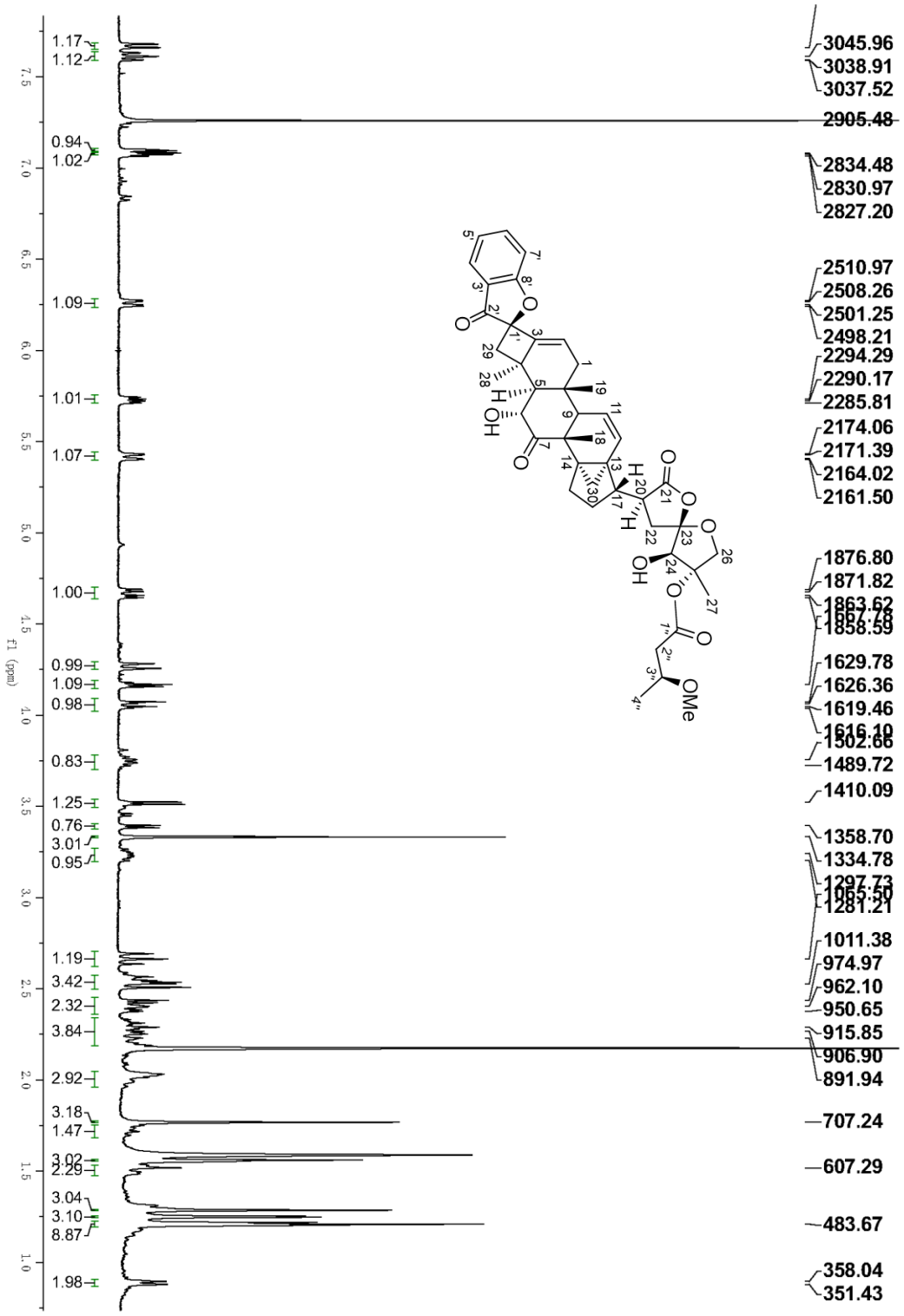

Figure S28. ^{13}C NMR spectrum of phainanoid H (**3**) in $CDCl_3$

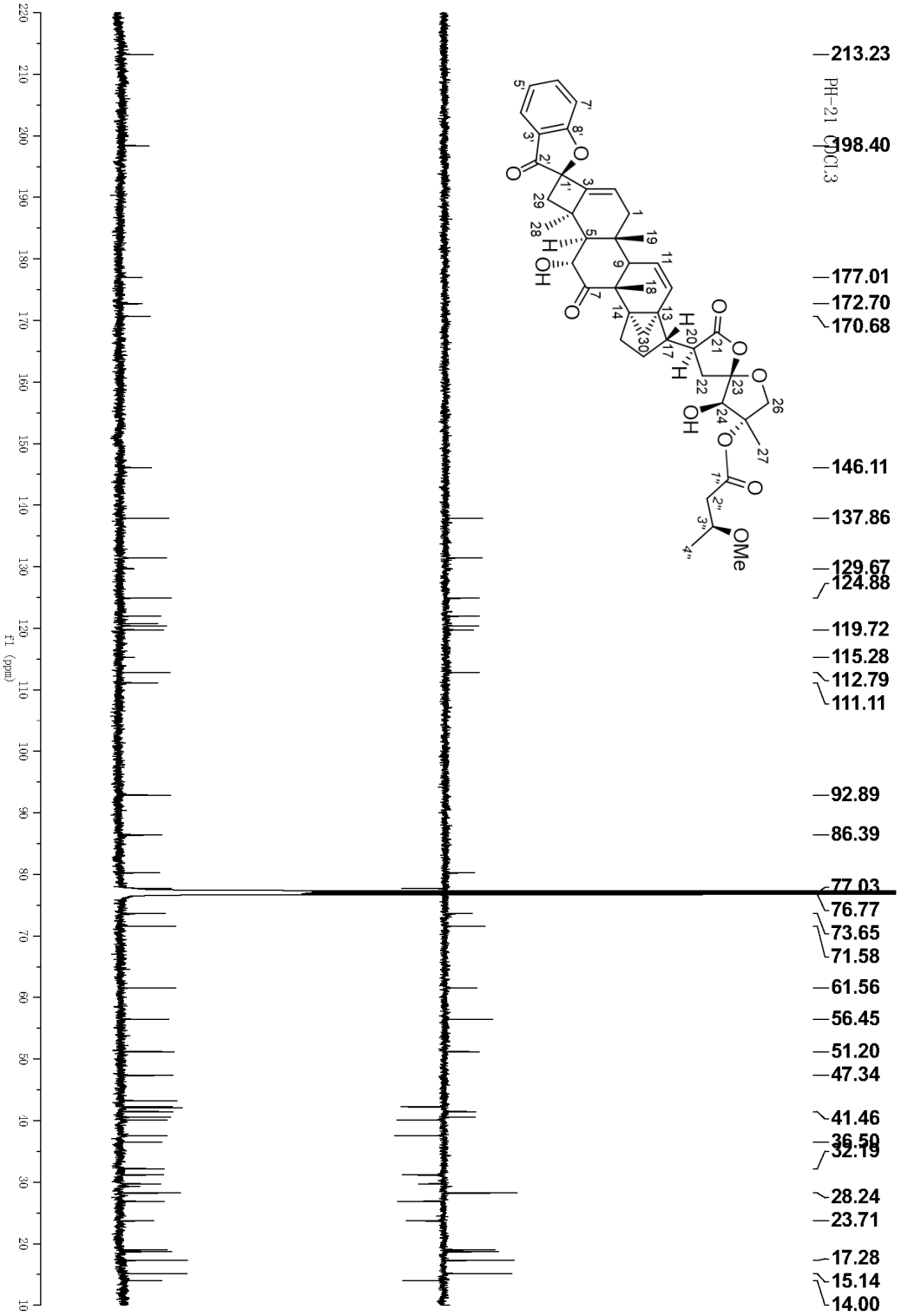

Figure S29. HSQC spectrum of phainanoid H (**3**) in $CDCl_3$

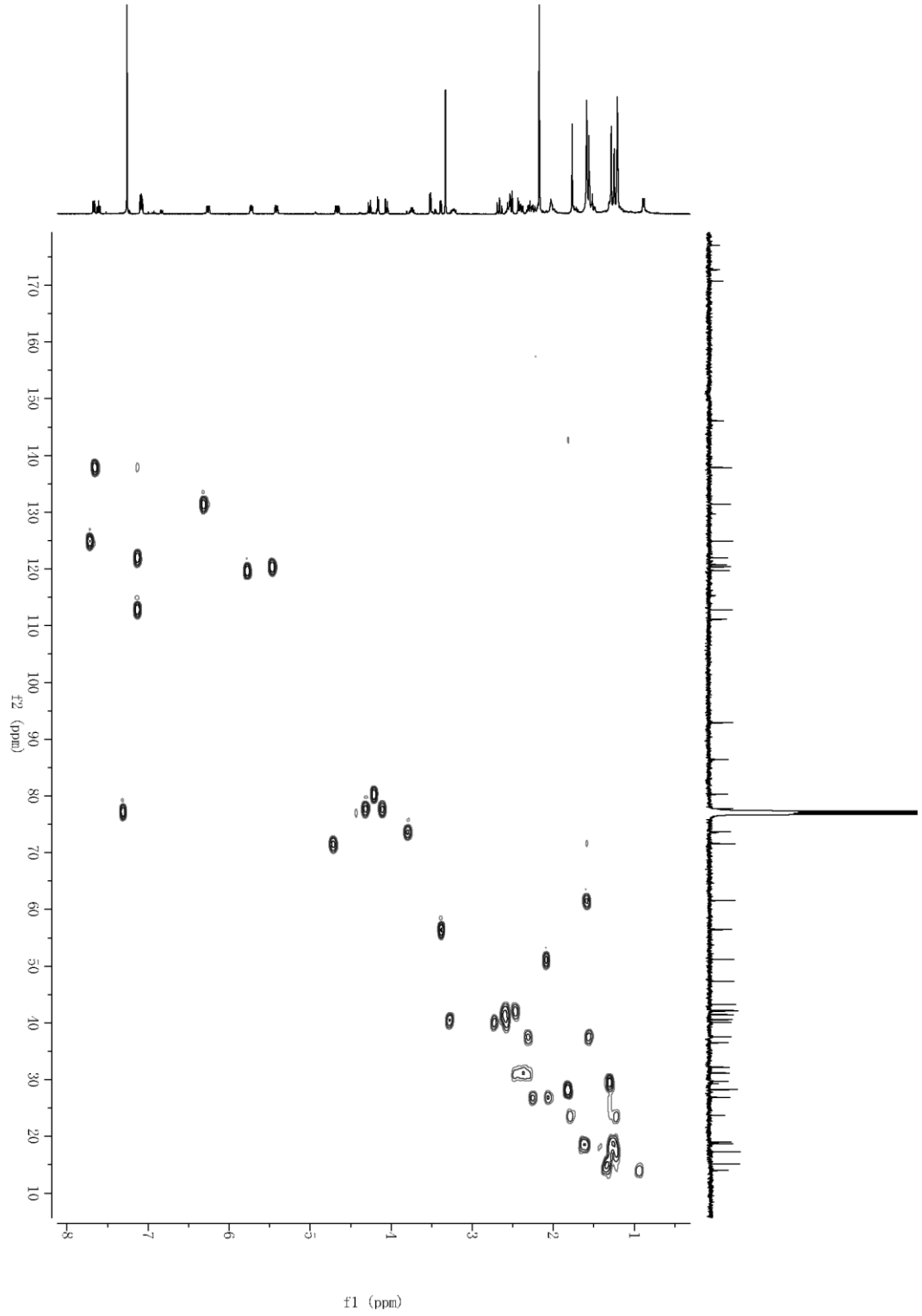

Figure S30. HMBC spectrum of phainanoid H (**3**) in $CDCl_3$

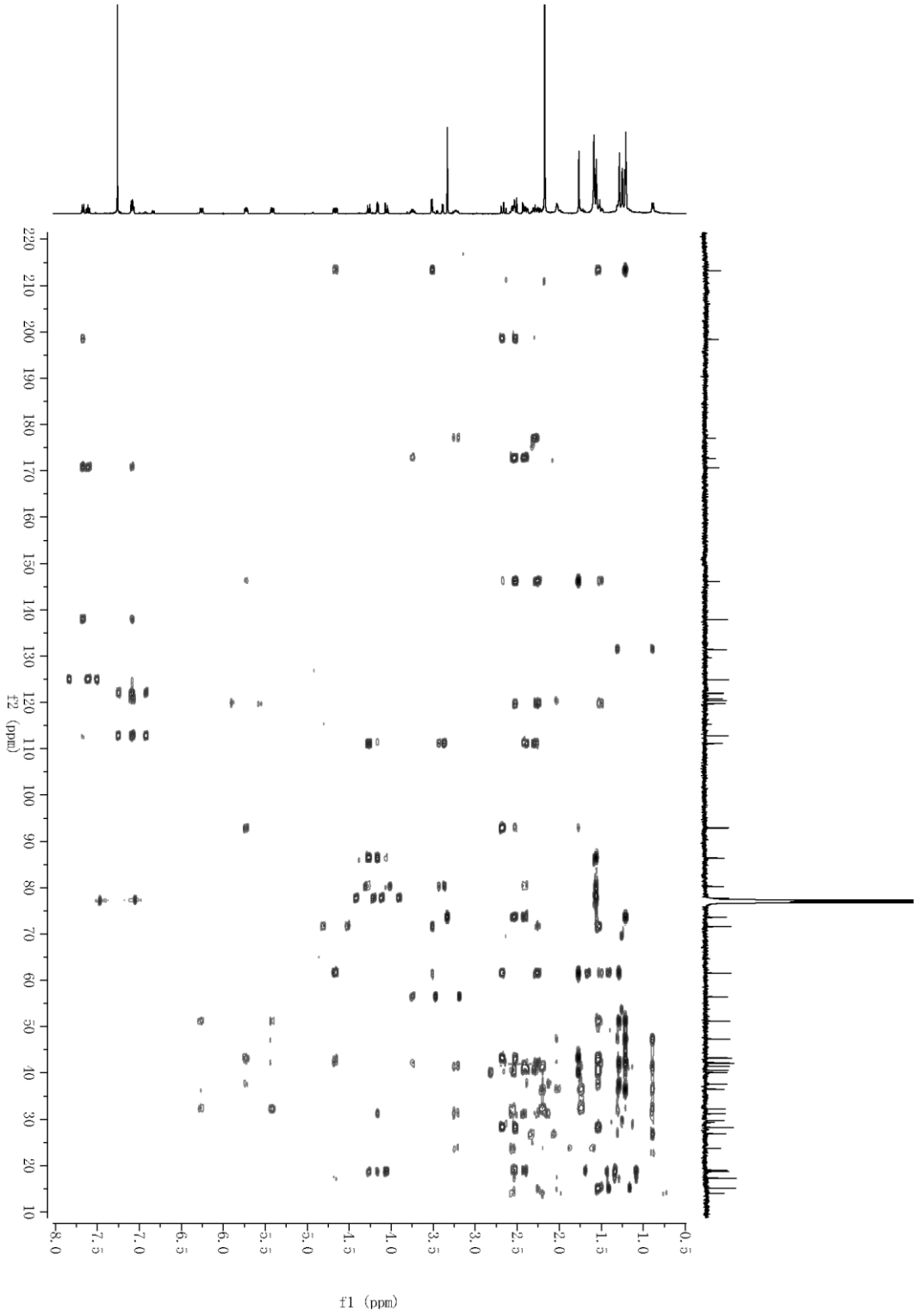

Figure S31. $^{1}H–^{1}H$ COSY spectrum of phainanoid H (**3**) in $CDCl_3$

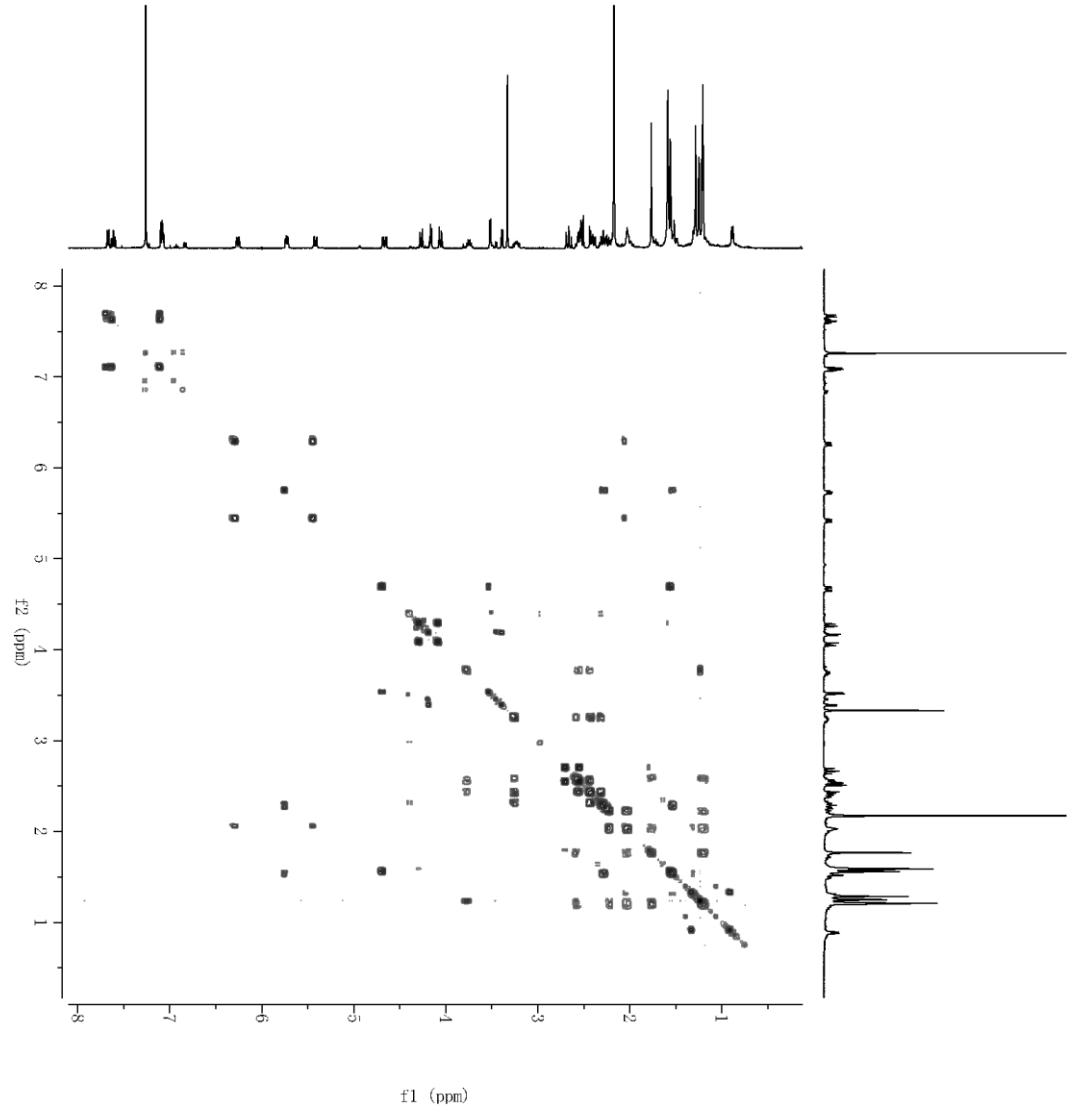

Figure S32. ROESY spectrum of phainanoid H (**3**) in $CDCl_3$

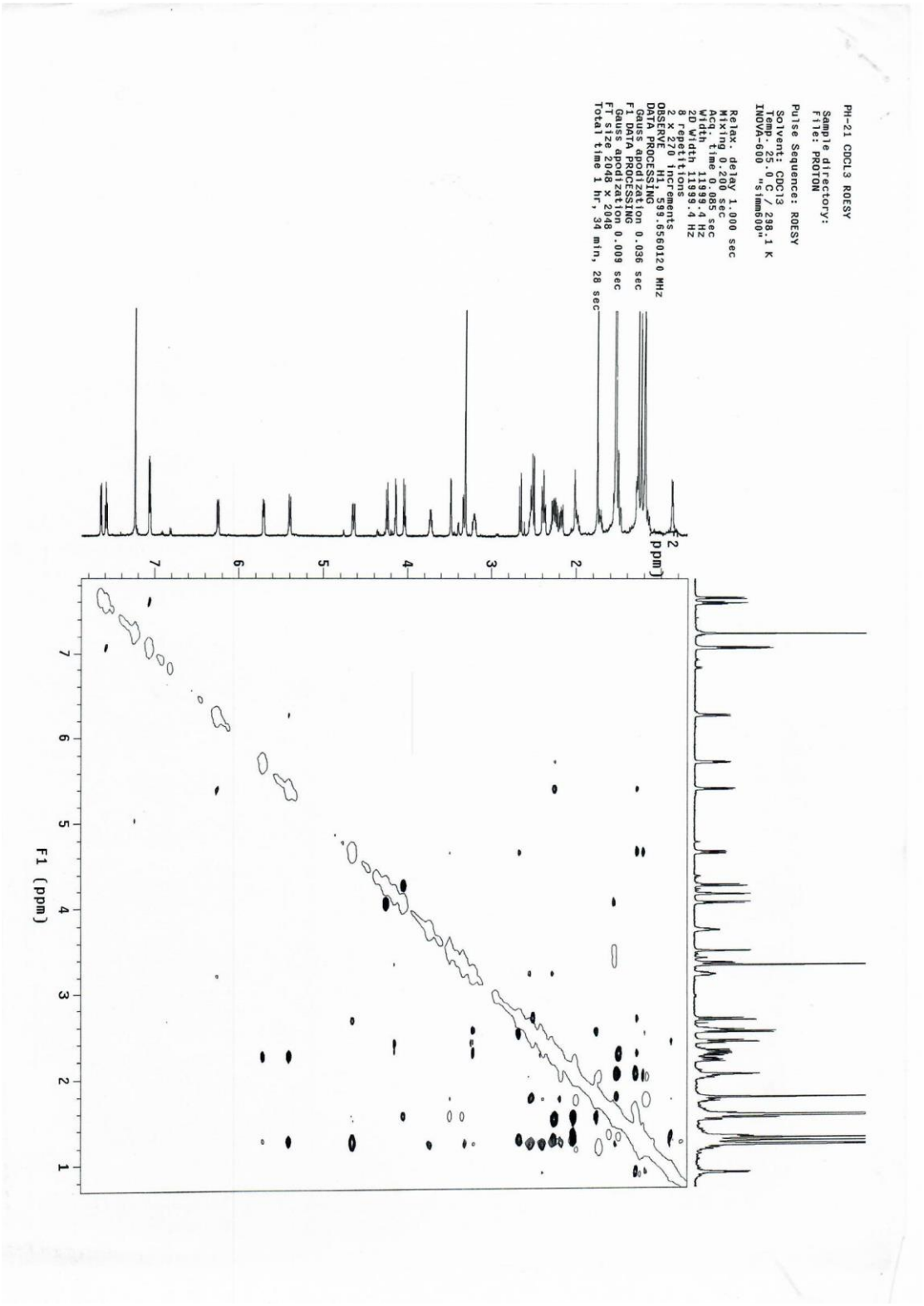

Figure S33. ESI(+)MS spectrum of phainanoid H (**3**)

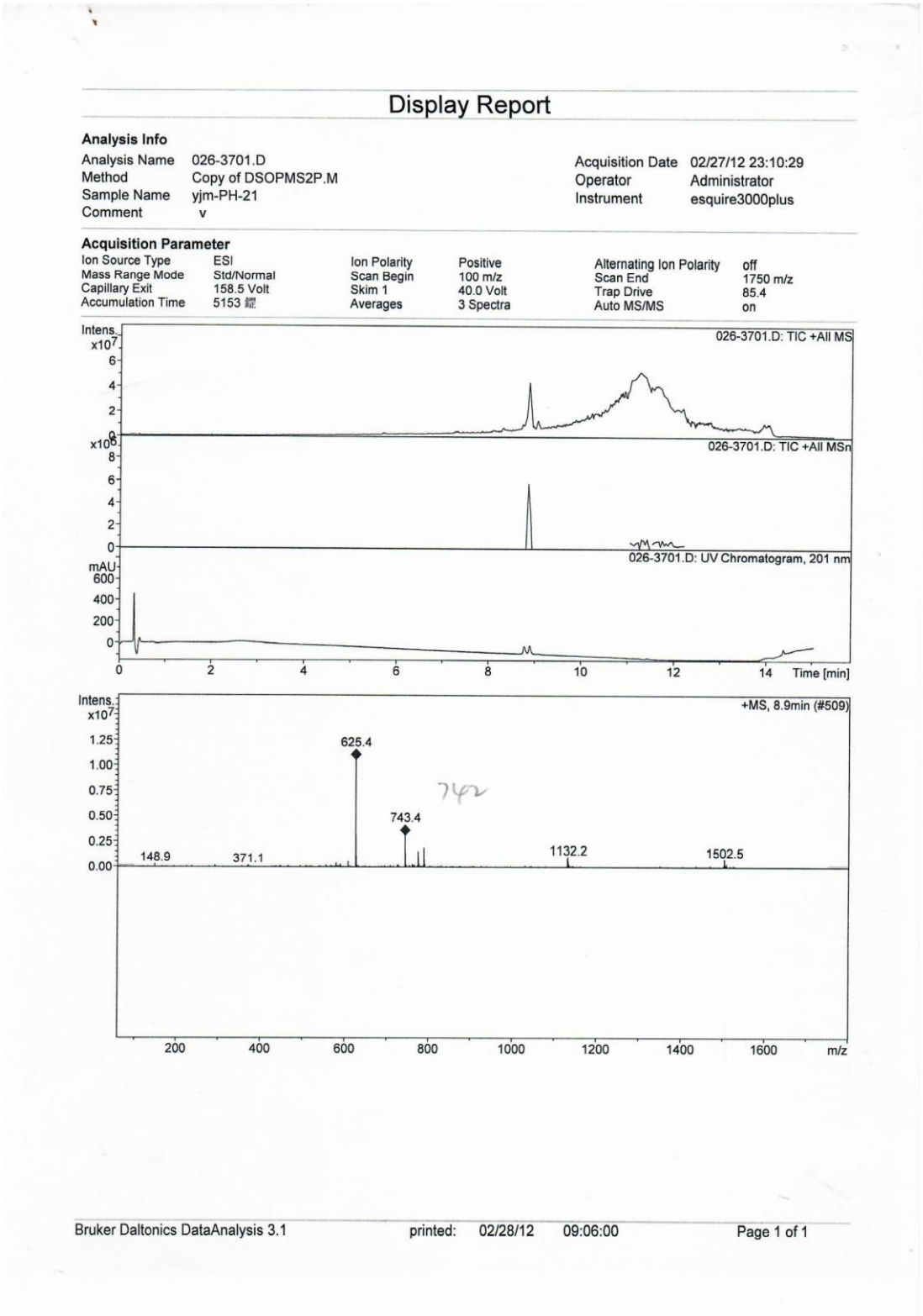

Figure S34. ESI(−)MS spectrum of phainanoid H (**3**)

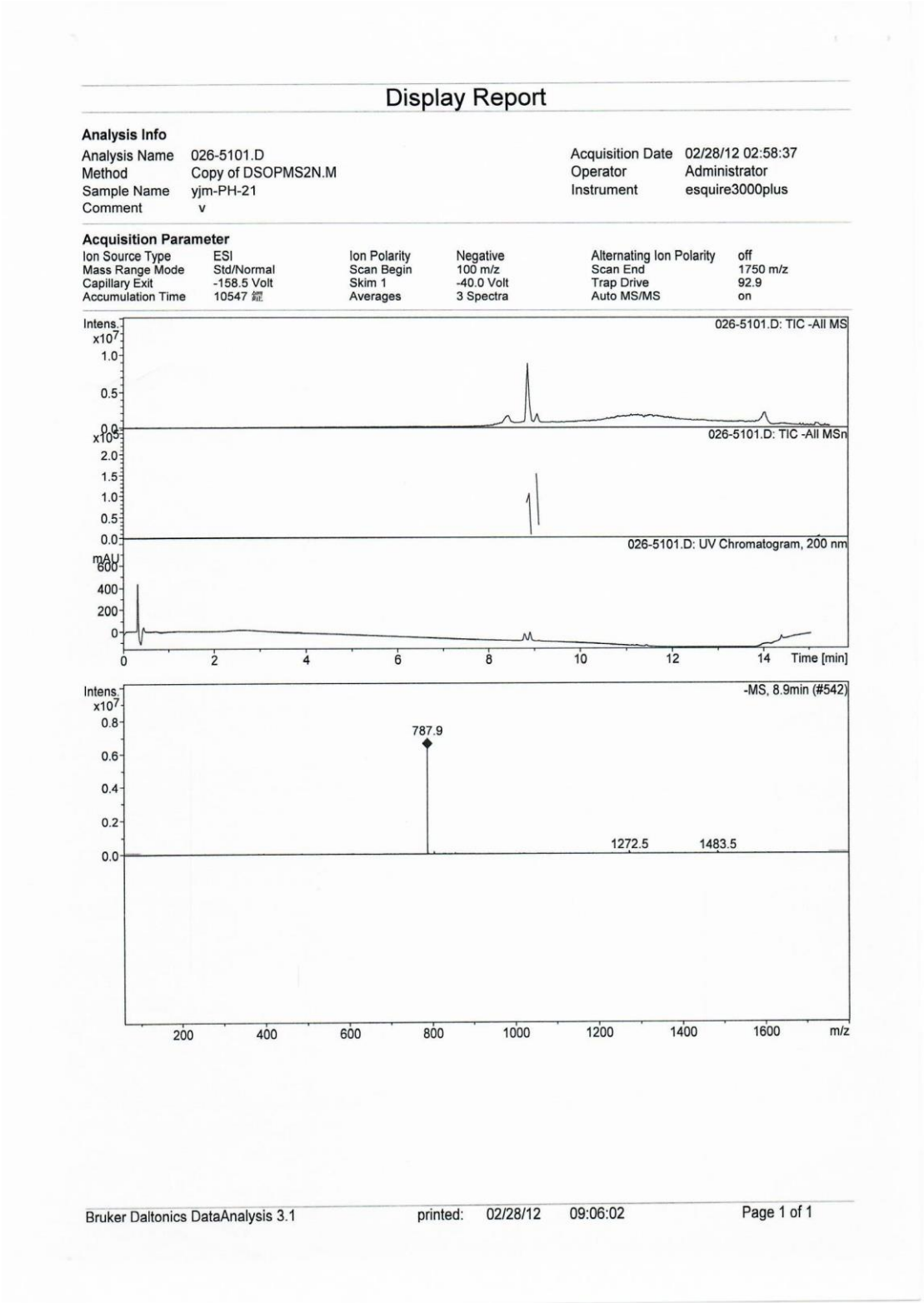

Figure S35. HRESI(+)MS spectrum of phainanoid H (**3**)

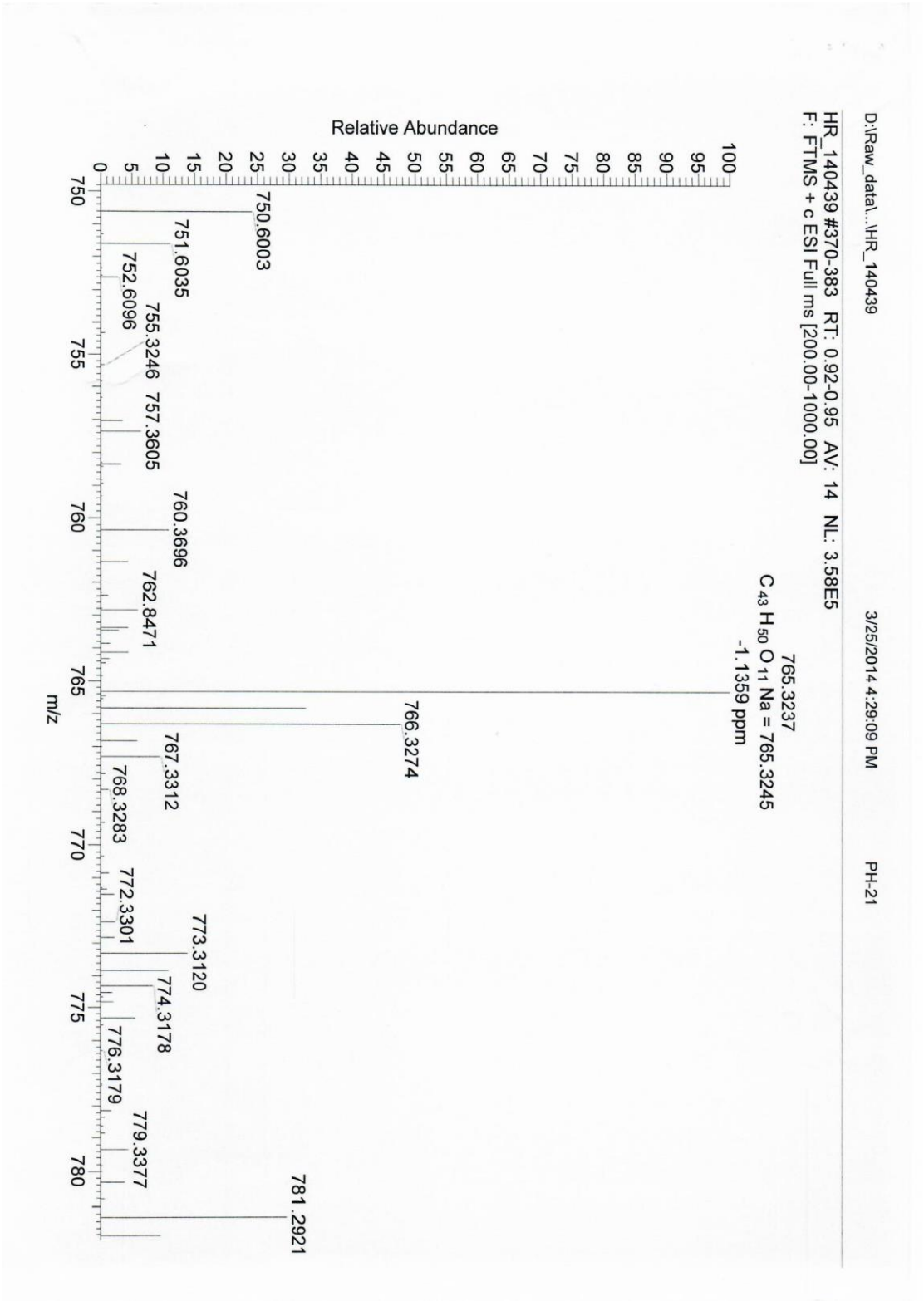

Figure S36. IR spectrum of phainanoid H (**3**)

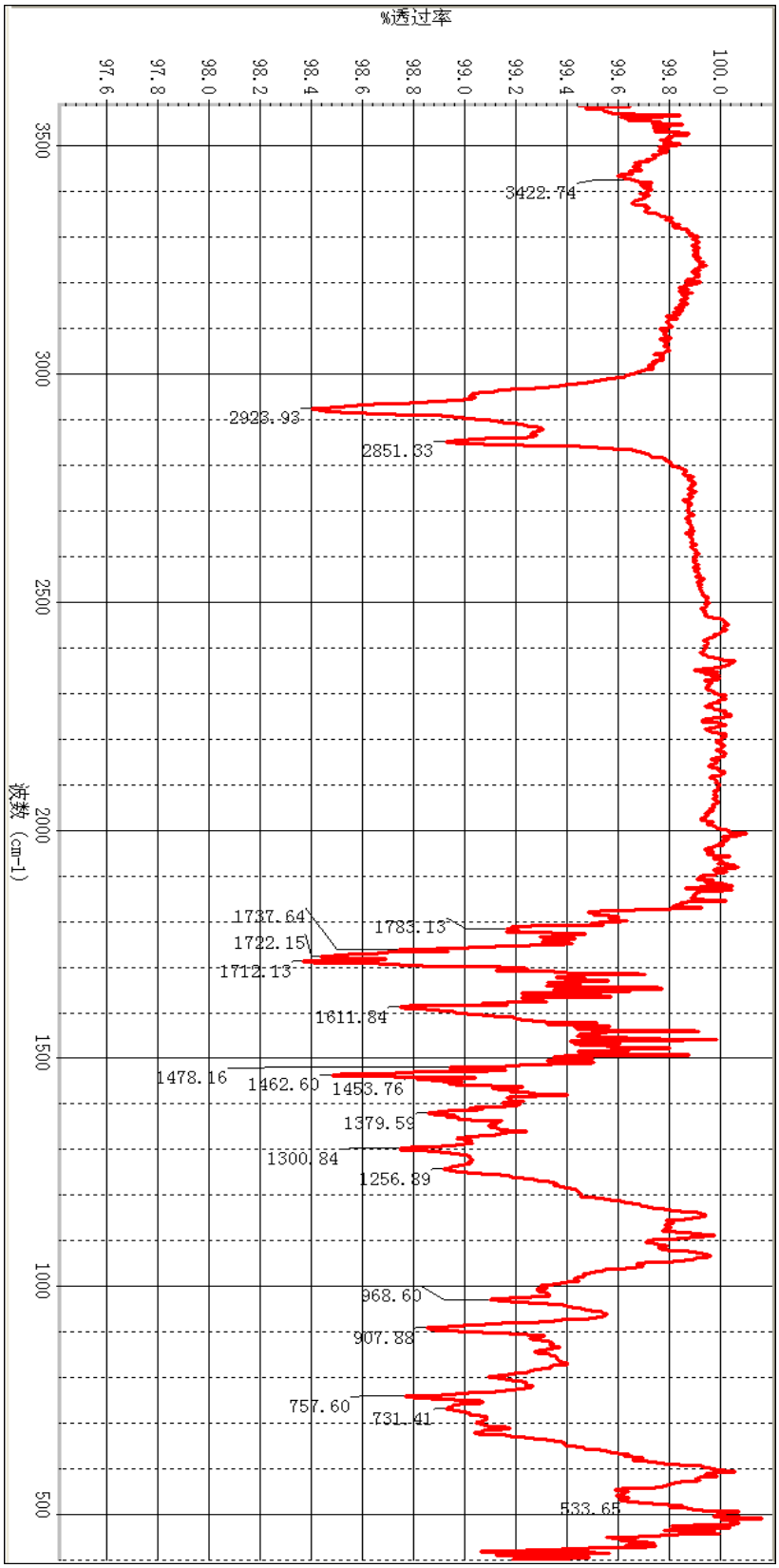

Figure S37. ^{1}H NMR spectrum of phainanoid I (**4**) in $CDCl_3$

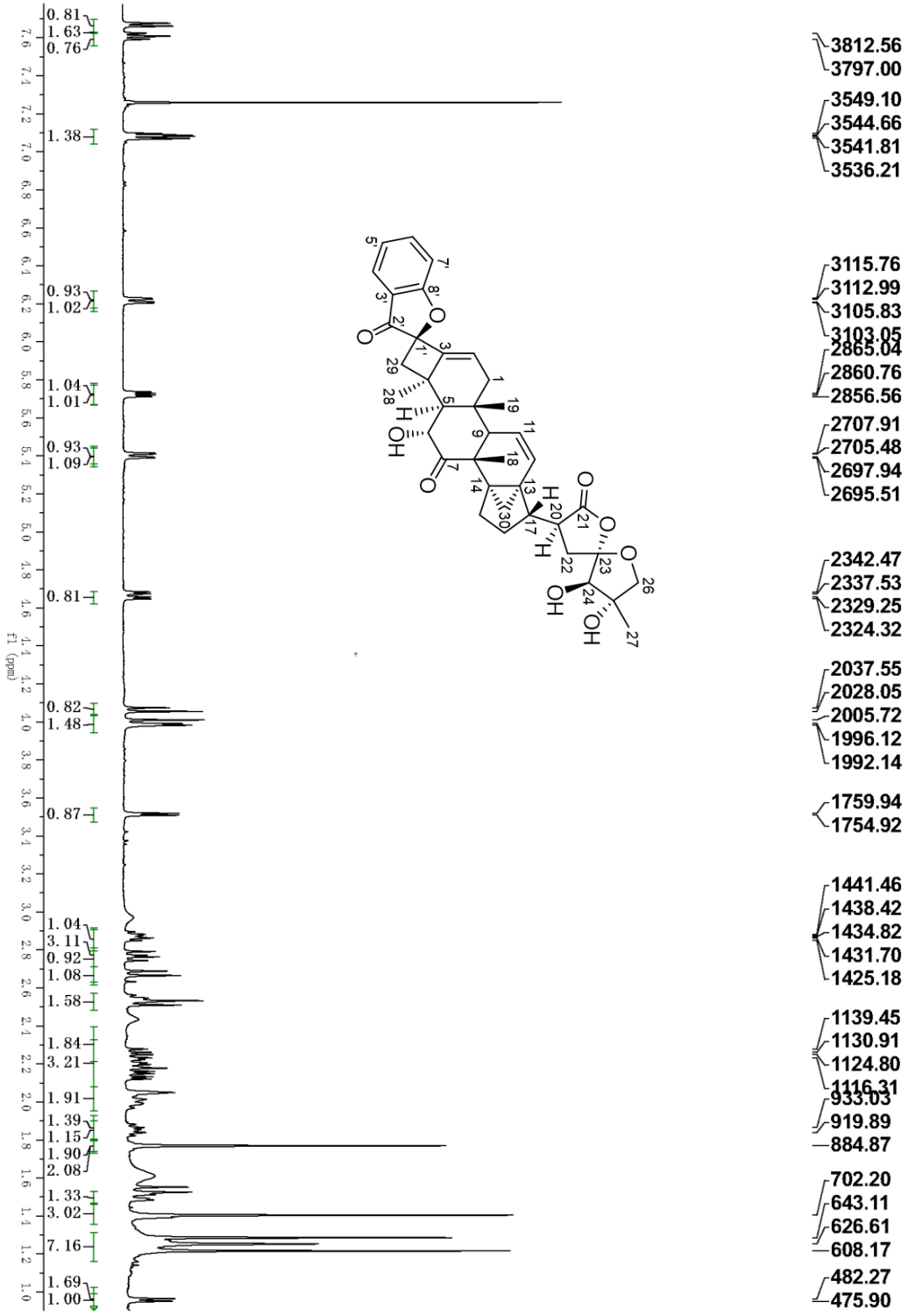

Figure S38. ^{13}C NMR spectrum of phainanoid I (**4**) in $CDCl_3$

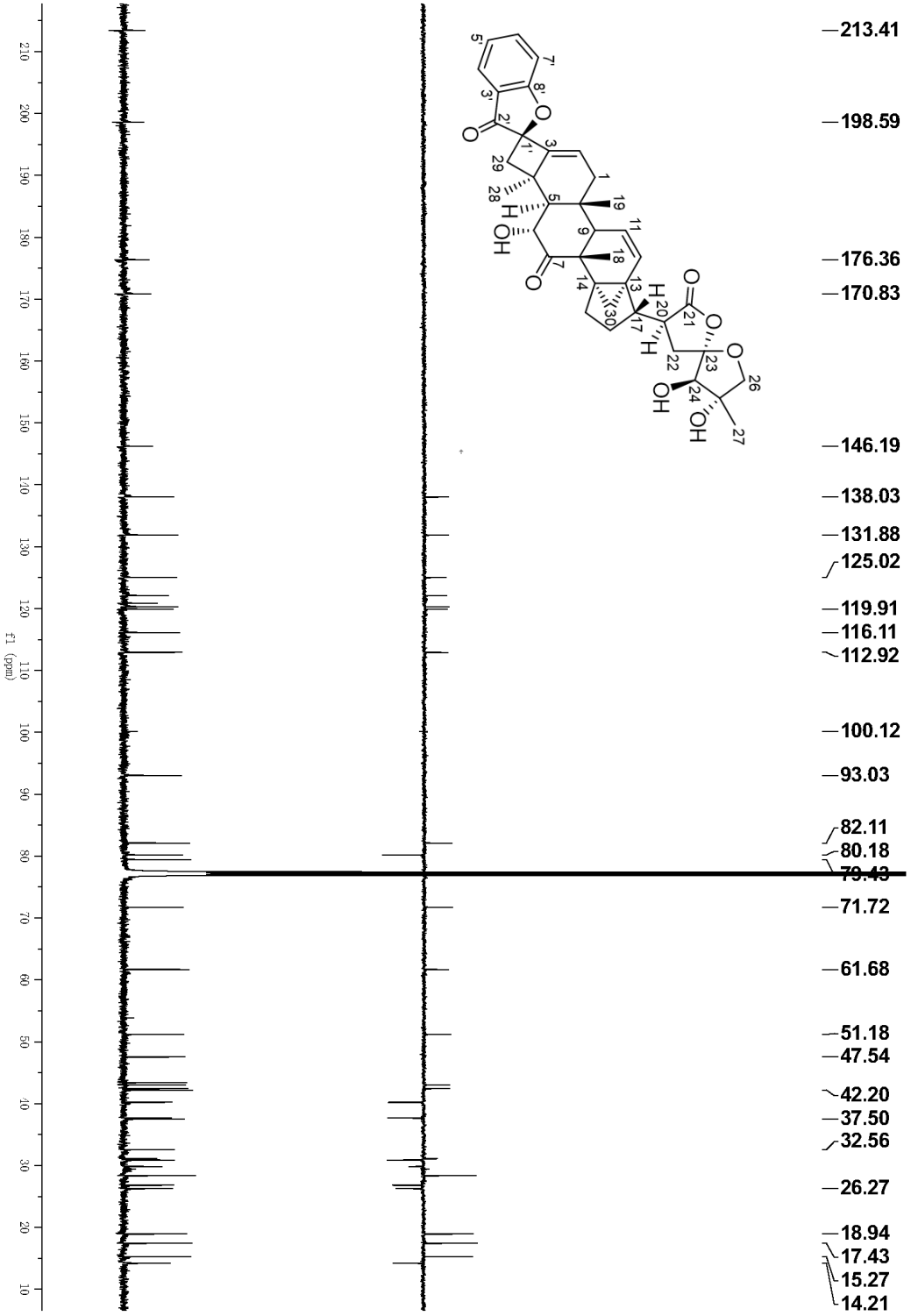

Figure S39. HSQC spectrum of phainanoid I (**4**) in $CDCl_3$

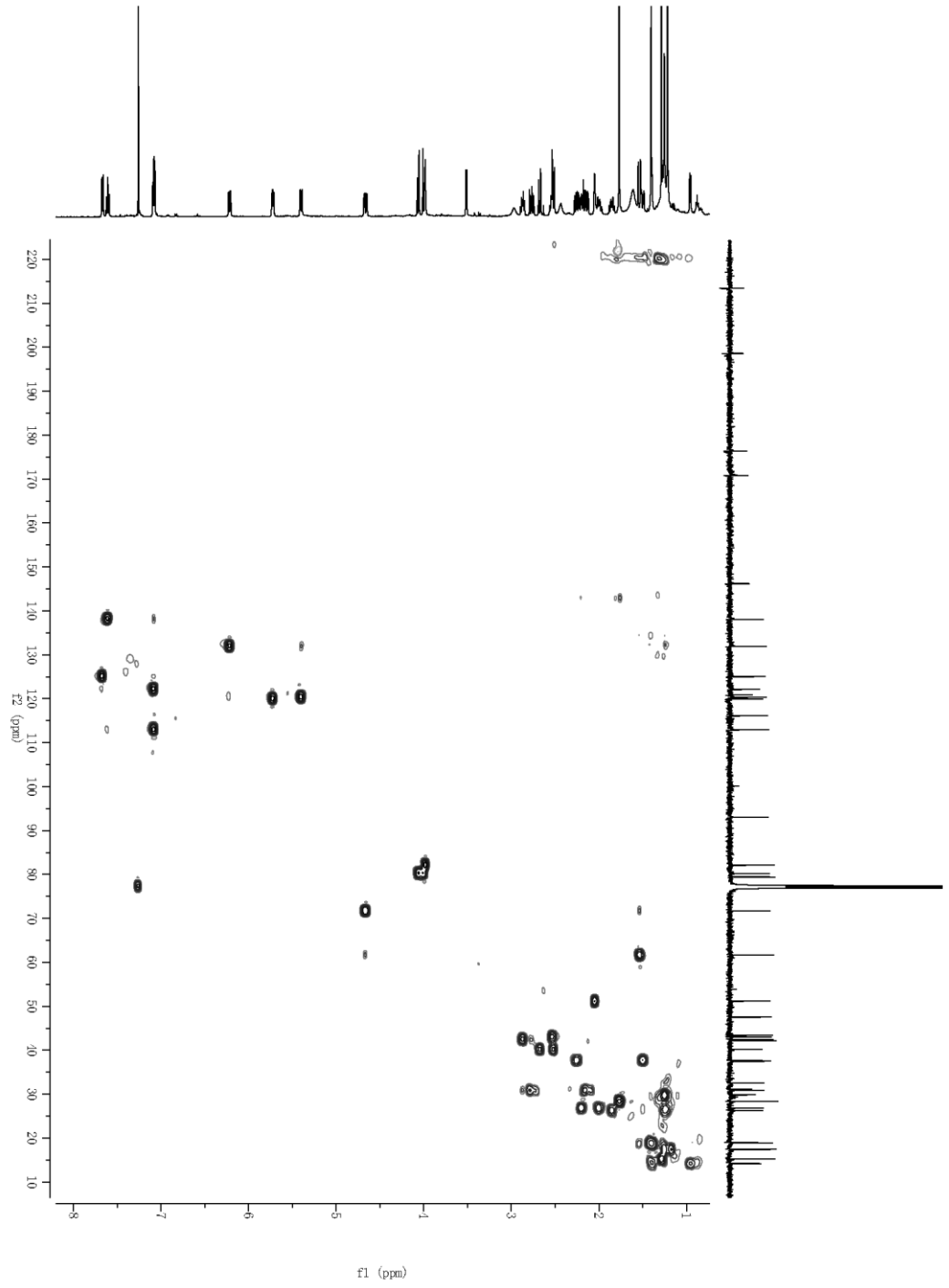

Figure S40. HMBC spectrum of phainanoid I (**4**) in $CDCl_3$

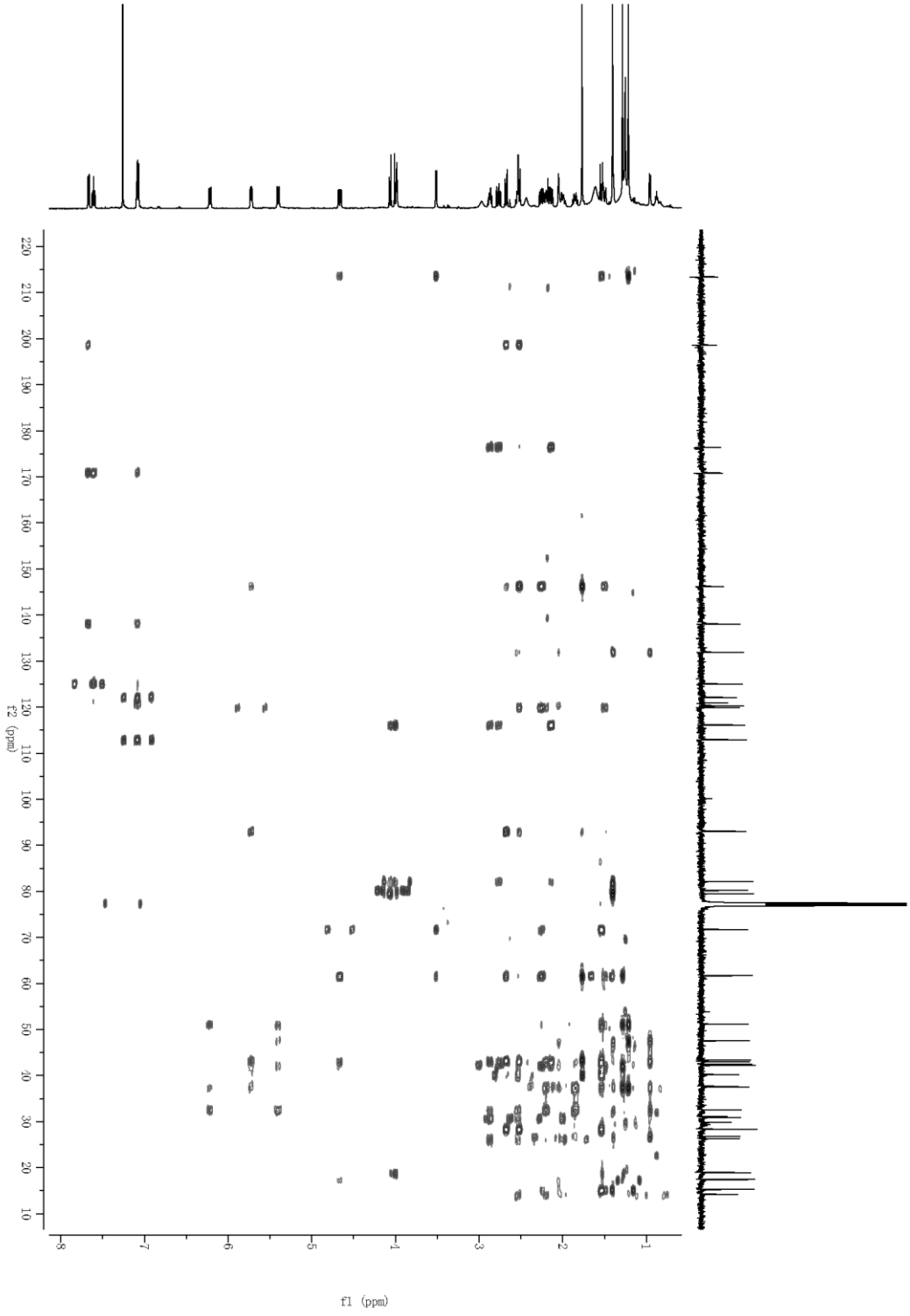

Figure S41. $^{1}H–^{1}H$ COSY spectrum of phainanoid I (**4**) in $CDCl_3$

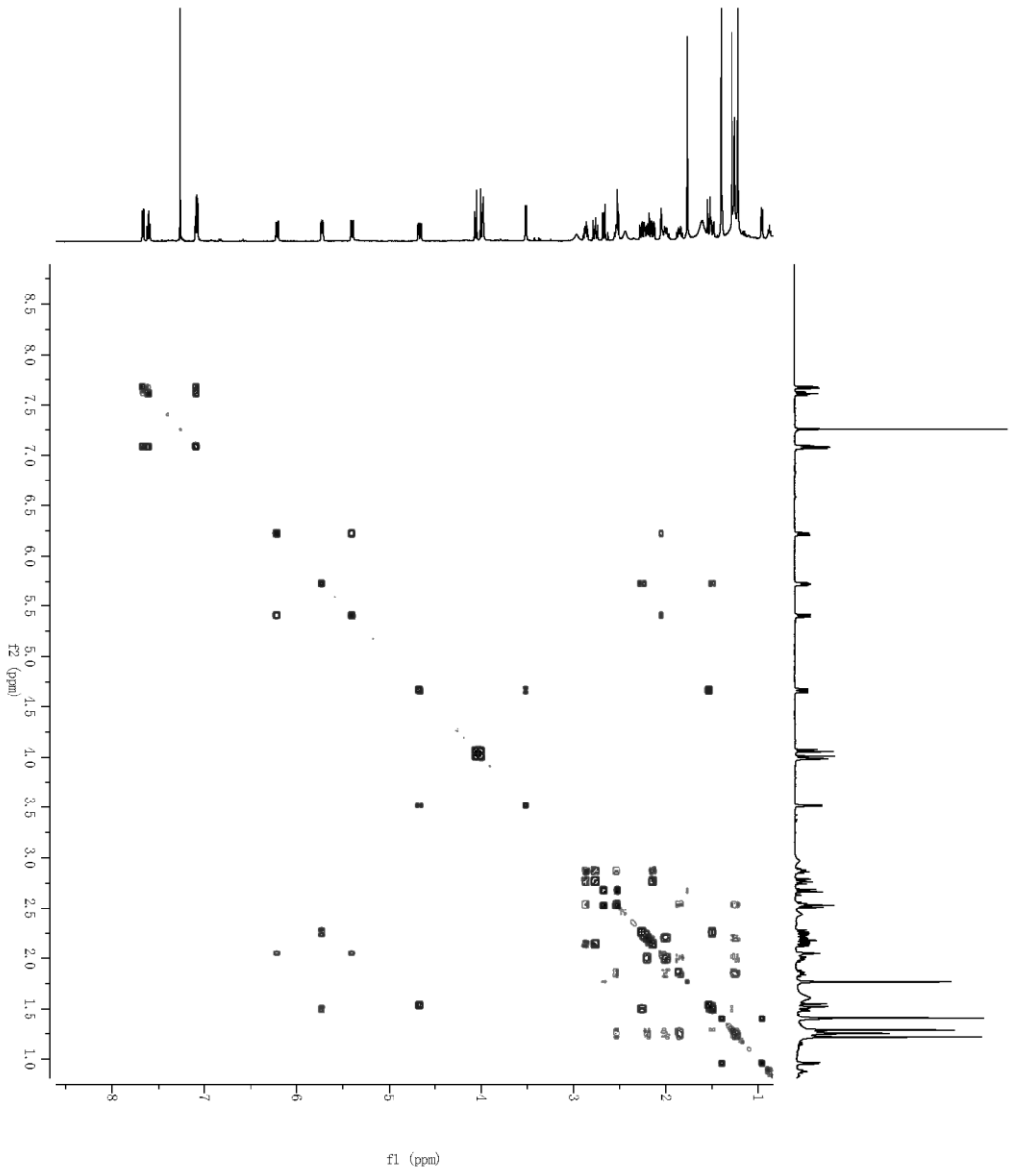

Figure S42. ROESY spectrum of phainanoid I (**4**) in $CDCl_3$

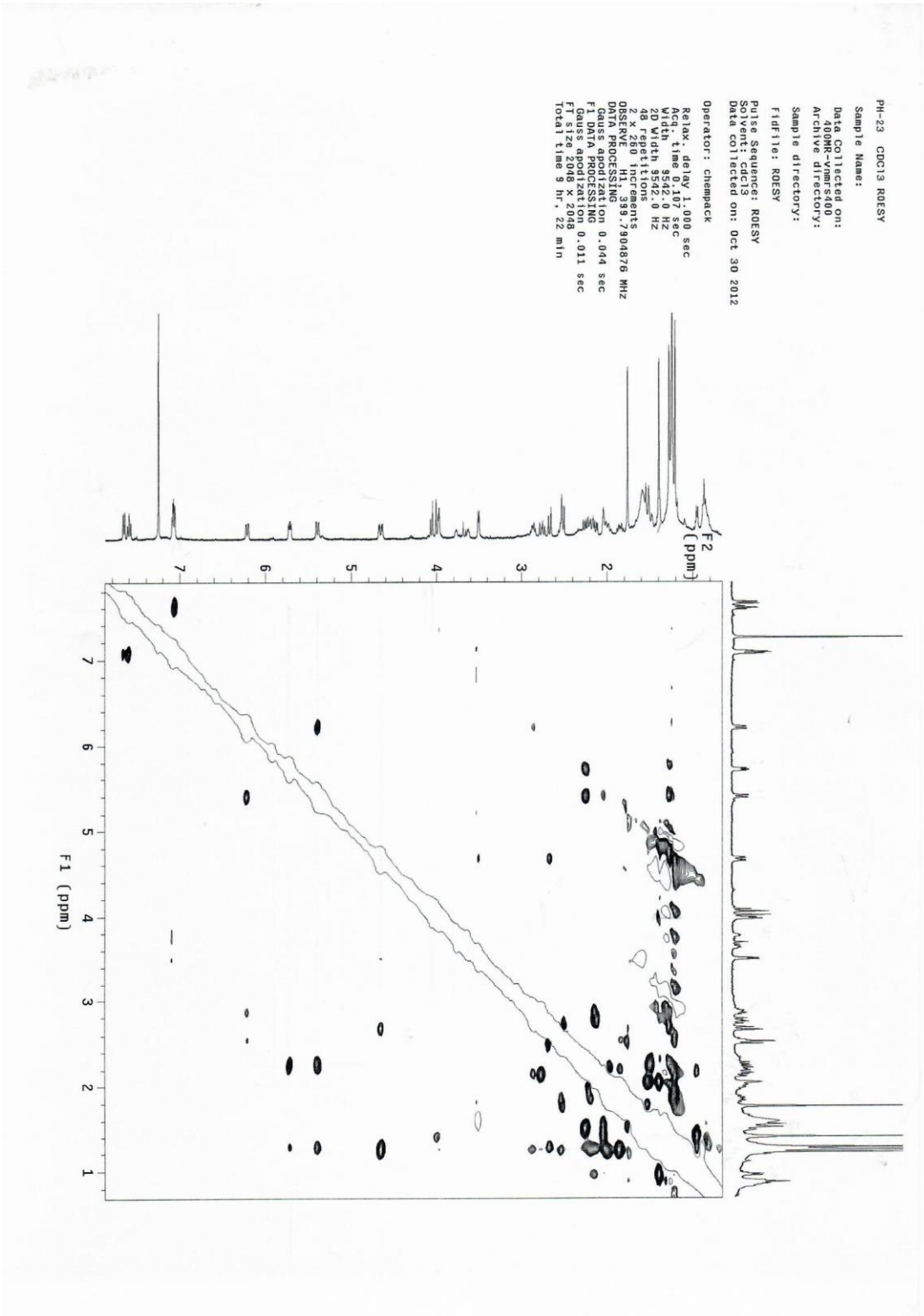

Figure S43. ESI(+)MS spectrum of phainanoid I (**4**)

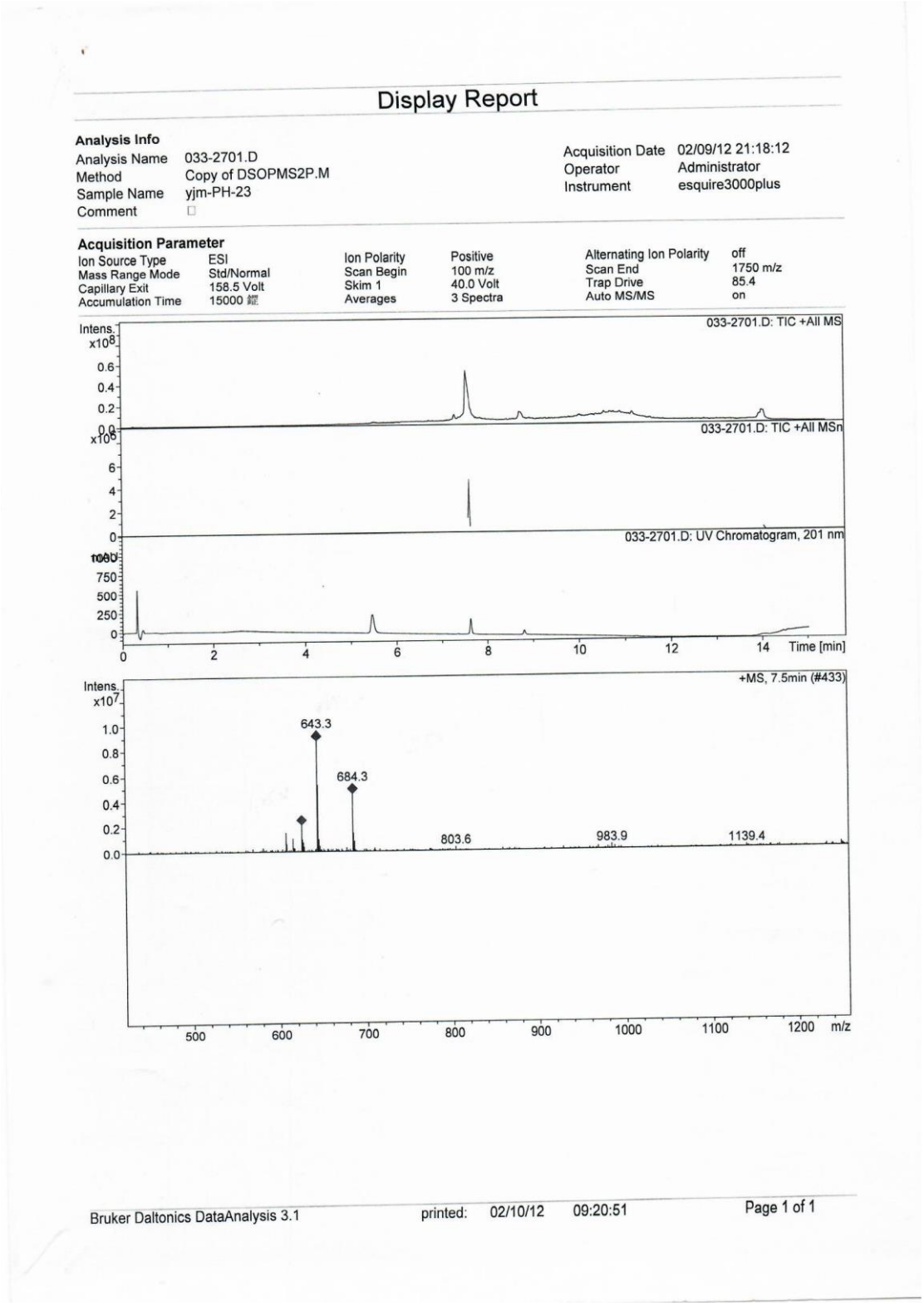

Figure S44. ESI(–)MS spectrum of phainanoid I (**4**)

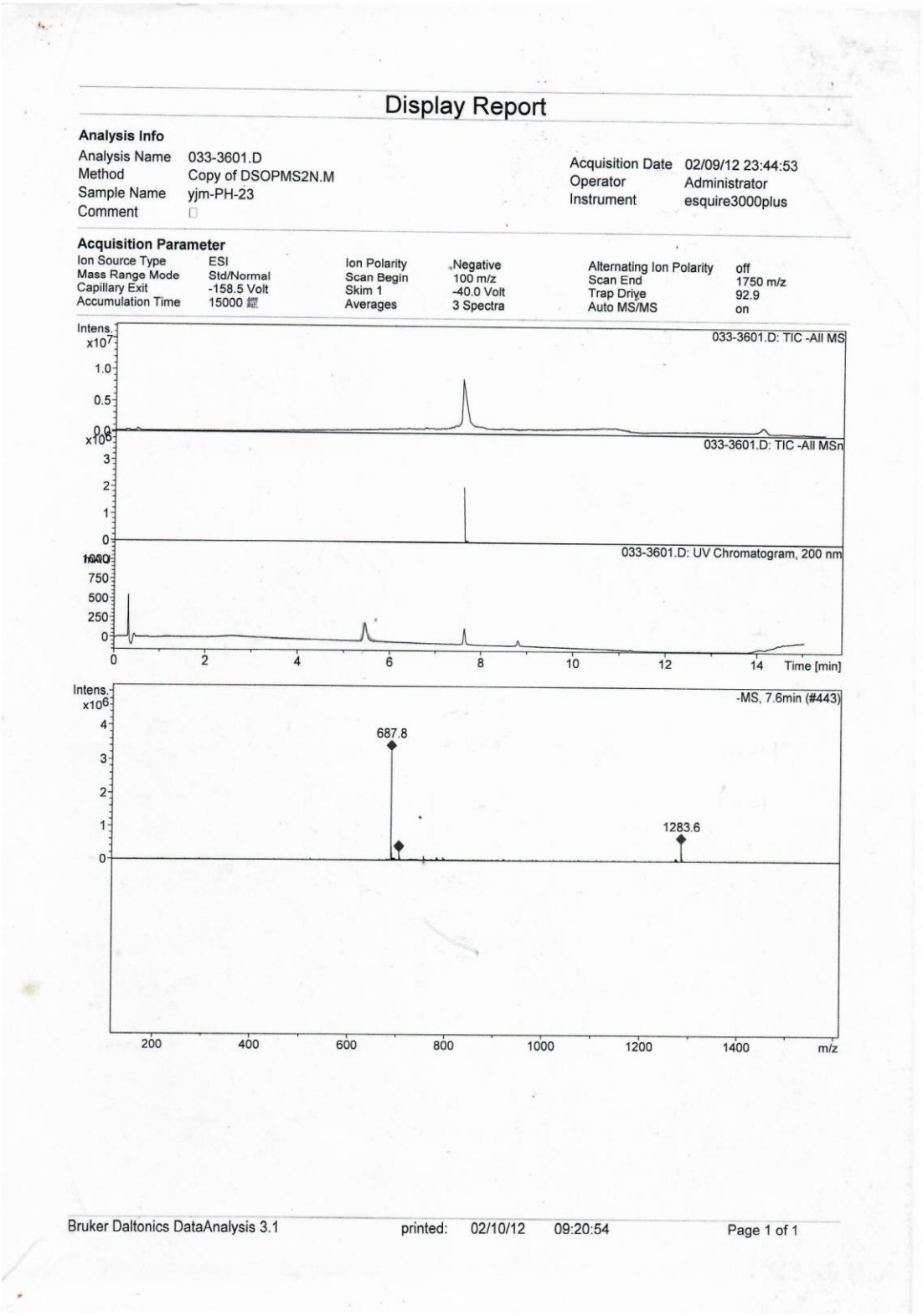

Figure S45. HRESI(–)MS spectrum of phainanoid I (**4**)

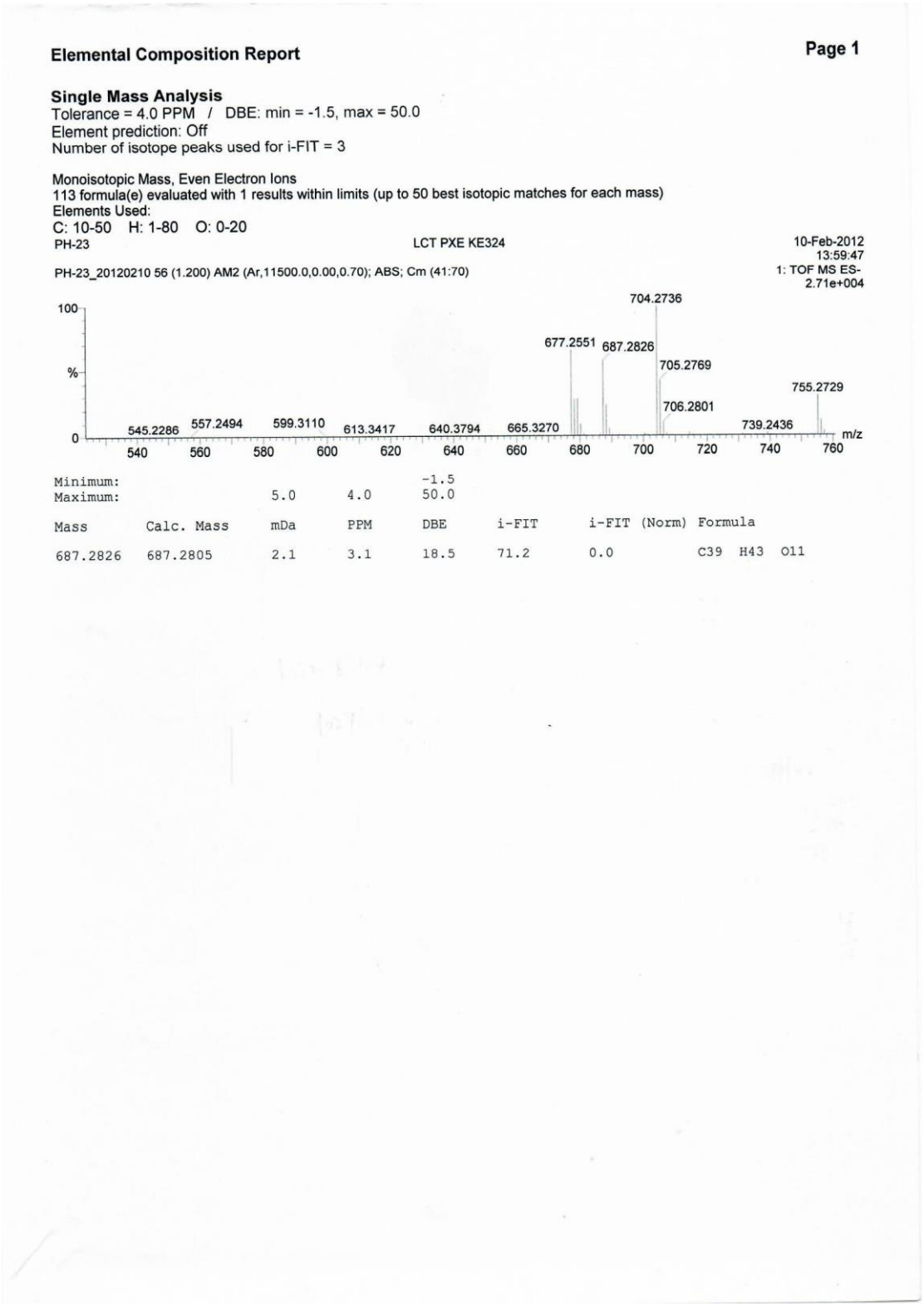

Elemental Composition Report Page 1

Single Mass Analysis
Tolerance = 4.0 PPM / DBE: min = -1.5, max = 50.0
Element prediction: Off
Number of isotope peaks used for i-FIT = 3

Monoisotopic Mass, Even Electron Ions
113 formula(e) evaluated with 1 results within limits (up to 50 best isotopic matches for each mass)
Elements Used:
C: 10-50 H: 1-80 O: 0-20

PH-23 LCT PXE KE324 10-Feb-2012 13:59:47

PH-23_20120210 56 (1.200) AM2 (Ar,11500.0,0.00,0.70); ABS; Cm (41:70) 1: TOF MS ES- 2.71e+004

Minimum:				-1.5			
Maximum:		5.0	4.0	50.0			
Mass	Calc. Mass	mDa	PPM	DBE	i-FIT	i-FIT (Norm)	Formula
687.2826	687.2805	2.1	3.1	18.5	71.2	0.0	C39 H43 O11

Figure S46. IR spectrum of phainanoid I (**4**)